Library
UTIG Tech. Report # 43

AGE, DEPTH, AND RESIDUAL DEPTH ANOMALIES IN THE NORTH PACIFIC: IMPLICATIONS FOR THERMAL MODELS OF THE LITHOSPHERE AND UPPER MANTLE

by

Miriam Renkin*

and

John G. Sclater*

*University of Texas, Austin, Institute for Geophysics
4920 North I.H. 35, Austin, Texas 78751

ABSTRACT

We present an empirical basement depth versus age relation for the North Pacific Ocean, based on the statistical treatment of an oceanwide gridded data set. The SYNBAPS bathymetry was averaged into half degree intervals and corrected for the effects of sediment loading. The resulting basement depths were plotted against ages determined from a revised isochron chart based on a recent compilation of magnetic lineations and various published plate reconstructions.

On crust older than 80 Ma, the depths are skewed to the shallow side of the depth versus age distribution by large numbers of seamounts. Therefore the mean and standard deviations are not useful representations of the data. A more appropriate representation is the mode (or greatest concentration of points) and contours around the mode. The contours around the mode show that most ocean floor increases in depth with the square root of age out to crust of 80 Ma. Beyond this the majority of the data oscillates about a line that remains essentially constant as the age increases. Approximately 56% of all the data points lie within a $\pm$ 300 m band about the mode.

If the sediment thickness data in the older basins of the western North Pacific is correct then the flattening of the depths favor a model in which extra heat is supplied to the base of the lithosphere on older ocean floor. Residual depth anomalies were calculated by removing the depths predicted by such a model. These anomalies correlate with bathymetric features and occur predominantly on crust of 120 and 160 Ma. They account for the rises in the mode at these two ages.

The overall subsidence of the ocean floor can be accounted for by the cooling of a thermo-mechanical boundary layer. Correlations between geoid height and depth are evidence that many of the residual depth anomalies result from convective plumes which reset the thermal structure of the lithosphere. It is possible that this process observed at different times after the initial resetting of the isotherms may account for many of the depth anomalies in the western North Pacific.

INTRODUCTION

Oceanic plate is created by the intrusion of hot molten material at a spreading center. This material attaches itself to the plate and moves away from the zone of intrusion as more material is emplaced. The newly created oceanic lithosphere cools and contracts which gives rise to a correlation between ocean depth and age and heat flow and age, the ocean floor being shallower and hotter near a spreading center and deeper and colder in older regions. Thus, the relationship between ocean basement depth and age ideally represents the cooling behavior of oceanic lithosphere. Well defined relations between depth and age and heat flow and age can be used to constrain thermal models of the oceanic lithosphere.

In particular, the relation between depth and age allows the differentiation between models where the lithosphere is to be considered a flat plate and others where it is assumed to cool like a simple rigid boundary layer. In addition, this relation permits the investigation of regional variations of depth about that predicted by models of lithospheric creation and cooling. Correlation of these regional variations of depth, known as residual depth anomalies, with the geoid field yields important constraints on the form of convection in the upper mantle.

Though there have been many attempts to examine the relation between depth and age in the North Pacific (for example, Sclater and Franchetean (1970), Sclater et al., (1971), David and Lister, (1974), and Menard and Dorman (1971)), only two, by Parsons and Sclater (1977) and Schroeder (1984), have examined the relation for all ages. From these two studies, it is accepted that the depth of oceanic basement increases as the square root of age for the first 80 million years and then flattens to a near constant value as the crust gets older. However, both studies are incomplete. As they wished to limit themselves to region of as deep a depth as possible of known age, Parsons and Sclater (1977) considered only a small area in the western Pacific. Schroeder (1984), on the other hand, presented a much more comprehensive treatment. However, because of problems with estimating age he also left out a substantial area in the western and central Pacific. Further, as he concentrated only on the simple cooling model, he presented his data almost entirely as depth against the square root of age. This method of analysis reduces the visual effect of depth variations in the older regions and he was unable to examine his observed flattening of the depth with age in the older regions in any detail. Finally, he had to construct his $1^{o}x1^{o}$ averages from contour charts as no digital data base existed at the time he started his analysis.

Recently new developments have taken place in our understanding of the tectonic history of the western North Pacific. In addition, a new digital data base SYNBAPS has been made available to the scientific community (Van Wykhouse, 1973).

In this current study, we use recent theories on the the tectonic history of the western North Pacific to develop an isochron chart for the whole area. We use the SYNBAPS bathymetry data compilation (Van Wykhouse, 1973) to compile $1/2 \times 1/2^{o}$ average depths for the entire North Pacific. The data are corrected for the loading effect of sediment using the method of Crough (1983) to arrive at basement depths for the same region. We examine the relation between depth and age and justify using the mode and contour intervals about the mode as representations of the information because of the highly skewed nature of the data on old oceanfloor. Using this representation, we select a preferred model for the cooling lithosphere and from it construct a chart of residual depth anomalies. We compare these anomalies with the geoid field. Finally, we discuss the implications of this comparison and the overall depth versus age relation, away from areas of anomalous depth, for models of lithospheric cooling and mantle covection.

A REVISED ISOCHRON CHART

Sclater et al. (1980) and Larson et al. (1984) constructed isochron charts of the North Pacific. These charts are very general in nature and permitted these authors to avoid the problem of constructing a tectonic history in the quiet zone. As we wish to examine the older ocean floor in some detail, we cannot avoid determining ages in these zones. In this section, we use the magnetic lineation compilation of Cande et al. (1986), basement ages from Deep Sea Drill Project holes, and various published theories and interpretations to construct a revised isochron chart for both the western and eastern North Pacific.

The North Pacific Ocean basin contains both the youngest and the oldest oceanic crust in the world. The seafloor ranges in age from the presently forming crust along the East Pacific Rise and the Juan De Fuca and Gorda ridges to the supposedly mid-Jurassic crust (170-180 Ma) of the Mariana Basin. The Pacific plate, now the only major plate remaining in the North Pacific, formed in the mid-Jurassic. Adjacent to the Pacific plate were the Izanagi, Farallon, and Phoenix plates, which have all since been subducted or have been incorporated into modern plates.

Much of the tectonic history of the Pacific Ocean basin has been deduced by reconstructing identifiable magnetic lineations or individual anomalies. However, problems arise when attempting to define the age and tectonic history of the oceanic floor that formed during the "quiet zones", which are long intervals of normal polarity during the Jurassic and Cretaceous. The Jurassic quiet zone dates from some time before the first identifiable magnetic lineation M29 (160 Ma). The Cretaceous quiet zone spans from Mesozoic anomaly M0 (119 Ma) to Cenozoic anomaly 34 (84 ma). Also, areas where later mid-plate volcanism has obscured the original reversal pattern are difficult to define. The absence of dateable reversals makes it very difficult to deduce a model of the tectonic history, especially for times when major plate reorganizations took place.

In spite of these problems DSDP results, edifice dredging, analyses of bathymetry, and occasional seismic surveys have contributed to many published models for the early formation of the North Pacific Ocean basin in the quiet zones (e.g. Larson, 1976; Hilde et al., 1977; Rea and Dixon, 1983; Mammerickx and Sharman, in press). These models, in some cases, allow reasonable estimates of the age of the ocean floor in the quiet zones. These estimates were necessary for this study even though it is recognized that they may have significant errors.

This study used the magnetic lineation compilation of Cande et al. (in press) (Figure 1) and the time scale of Kent and Gradstein (in press) for the known ages. The age of the ocean floor was gridded in 1/2 degree intervals by extrapolating the lineations to the nearest 1 my isochron. For the quiet zones imaginary isochrons were drawn based on the published tectonic theories.

Reconstruction of the Quiet Zones

The published reconstructions for the quiet zones used here were presented by their authors as preliminary models because there are many unsolved problems in these areas. The interpretations used in this study (Larson, 1976; Hilde et al., 1977; Rea and Dixon, 1983) were considered to be the most comprehensive at the time this work was done.

The interpretation of Hilde et al. (1977) was used to construct isochrons for quiet zone A of Figure 1. They hypothesized that a single triple junction between the Izanagi, Farallon, and Phoenix plates (Figure 2) evolved into three triple junctions. The newly formed Pacific plate occupied the triangular area between them. Spreading on the Izanagi-Pacific, Farallon-Pacific, and Phoenix-Pacific ridges created the triangle of lineations, beginning with M29 (160 Ma), that remains on the Pacific plate today. Such a scenario is an over simplification since the configuration would probably be unstable in the early stages. However, with current data there is no support for an alternative history.

We created isochrons for the area by extrapolating the Izanagi-Pacific, Farallon-Pacific, and Phoenix-Pacific ridges back in time using the spreading rates measured between M25 and M29 (156 and 160 Ma). They meet at a point in the Mariana Basin estimated to be 174 Ma (Figure 2). A ridge jump has been added to the isochron pattern just east of the Mariana Trench to explain the offset along the fracture zone that cuts the Izanagi-Pacific lineations.

The area of quiet zone B (Figure 1) formed between the times of M25 and M0 (156 and 119 Ma), but few magnetic lineations have been found in this area because later mid-plate volcanism has obscured the original patern. The interpretation of Larson (1976) was used to construct isochrons for this area because it is the only interpretation that includes the fan shaped Magellan lineations (Larson, 1976; Tamaki et al., 1978).

The scenario of Larson (1976) begins at M25 time (156 Ma) when the Pacific-Farallon-Phoenix junction was a fault-fault-ridge triple junction (Figure 9 of Larson, 1976; note that he used a different time scale). Evidence for this is provided by one of the north-south fracture zones that appears to have been the eastern boundary of the Phoenix lineations at this time. Spreading along the Farallon-Phoenix ridge, between M25 and M14 (156-139 Ma), produced the east-west trending isochrons in area a of Figure 3 as well as all of the isochrons 139 Ma and older in areas b, c, and d (Figure 3). At M14 time (139 Ma) the triple junction jumped slightly eastward, as indicated by another more easterly trending north-south fracture zone in the Phoenix lineations, terminating the spreading in area a but continuing it in areas b, c, and d until M12 time (135 Ma). Larson (1976) suggests that the Farallon-Phoenix ridge trended more northwest-southeasterly during this period. At M12 time (135 Ma), the ridge that formed the Magellan lineations was created.

The fan shaped Magellan lineations open "in the opposite sense" (Larson, 1976) to the M12-M4 (135-126 Ma) Hawaiian lineations. Thus, they could not have formed by a simple rotation of the Pacific-Farallon spreading center. The Magellan spreading center, therefore, became the boundary between a new set of plates. Two triple junctions are required. Larson (1976) places the second triple junction at the eastern end of the Mid-Pacific Mountains. He suggests that this seamount studded plateau was formed on a slowly spreading ridge from M12-M4 (135-126 Ma) time. This origin for the Mid-Pacific Mountains is somewhat controversial (Winterer and Metzler, 1984). In the tectonic history of Larson (1976), the ridge to the west of the mountains is left unaccounted for.

The Magellan spreading center remained joined at its eastern end in a fault-fault-ridge triple junction with the Pacific(?)-Phoenix ridge and the Farallon-Phoenix ridge. The latter spreading center produced the isochron pattern in area e (Figure 3). The Magellan spreading center displaced and rotated the older patterns in areas c and d (Figure 3). On the western half of the Magellan lineations spreading stopped at M9 time (130 Ma), but it continued to M4 time (126 Ma) in the eastern half. A matching northern side for the eastern Magellan lineations (M4-M12, 126 Ma - 135 Ma) has been added north of M4 in area d (Figure 3).

Sometime between M4 and M0 time (126 and 119 Ma) this pattern of spreading stopped and reverted to the one currently observed for the eastern Pacific. Spreading on the Magellan lineations ended just after M4 time (126 Ma), while spreading on the Pacific(?)-Phoenix ridge stopped sometime after M1 (122 Ma). The change was arbitrarily chosen to occur just before M0 (at 120 Ma) in the vicinity of the Line Islands.

The Line Island chain trends at an angle to the pattern of approximately north-south lineations in the eastern Pacific. Because of the lack of observable anomalies in the Cretaceous quiet zone (between M0 and anomaly 34) the lineations cannot be traced as far west as the Line Islands. On the other hand, several of the major eastern Pacific fracture zones can be followed directly to the Line Islands but not beyond them (Mammerikx and Smith, 1985). Similarly, the Nova Canton Trough, which may mark the final position of the Pacific(?)-Phoenix ridge (Winterer, 1976), ends just west of the Line Islands and does not continue through them (Winterer and Mammerickx, 1976). The fracture zones dip toward the Line Island chain (Figure 3) but are not quite perpendicular to them. This indicates that, if spreading opened along the chain, it immediately changed its trend. The isochrons drawn in Figure 3 fan away from the island chain. The area just east of this chain is of variable age. The Line Islands are on a complex seamount chain (see Haggerty et al., 1982; Sager and Keating, 1984; Schlanger et al., 1984; Winterer, 1976; Jackson and Schlanger, 1976). The age of the oldest dredged volcanism is late Cretaceous and loading calculations (Watts et al., 1985) indicate that they formed on or near a spreading ridge.

The positions of the isochrons (Figure 3 and 4) were chosen using spreading rates determined from the relative motion vector triangles in Figure 9 of Larson (1976). Where there was disagreement, rates along conflicting sets of lineations were averaged.

Spreading in the quiet zone east of the Line Island chain (Figure 3) probably followed the simple north-south pattern seen in the rest of the eastern Pacific. However, both east and north of this chain, ridge jumps are necessary to explain the changes in offset across the major fracture zones. A specific case is the increase in offset along the Mendocino-Pioneer system that occurred during this period. Jumps by segments of the ridge may also explain the origin of the Pioneer and Murray Fracture Zones. Unfortunately, these jumps have not been located precisely. Consequently, they have been ignored and uniform spreading assumed between anomalies M0 and 34 (120 and 84 Ma) in determining the isochrons.

The interpretation of Rea and Dixon (1983) was used for quiet zone C of Figure 1 because it was the only interpretation available at the time that did not require strike-slip motion along the Emperor Trough (Farrar and Dixon, 1981; challenged by Gordon, 1982). In their scenario, (Figure 8 of Rea and Dixon, 1983) the Izanagi- (they refer to this plate as the "Bering" plate, but "Izanagi", given by Woods and Davies, 1982, is more commonly used) Farallon-Pacific triple junction continued to move north-eastward after M0 (119 Ma). Slow spreading around 110-100 Ma created the Hess Rise, a seamount-studded basalt plateau whose orientation suggests that it formed along the Pacific-Farallon ridge axis. At anomaly 34 (84 Ma) (Rea and Dixon used anomaly 32b, but the compilation of Cande et al., (1986), shows anomaly 34 at the bight) the triple junction and the Izanagi-Pacific and Izanagi-Farallon ridges may have entered a trench to the north and terminated. The result was a major plate reorganization. The new triple junction probably opened far to the east, around 45N, 170E.

Rea and Dixon (1983) pointed out that the existence of three separate systems of fracture zones, the Amlia-Adak system, the Mendocino-Pioneer system, and the Surveyor fracture zone, requires the existence of four plates in the region. To make the area between the Emperor Trough and the triple junction a new plate, they suggested that spreading continued at the Emperor Trough after the reorganization. Rea and Dixon (1983) named it the "Chinook" plate. They speculated that the Chinook Trough, an east-west trending feature stepped to the north by the Amlia-Adak fracture zone system, represents a scar of the opening of the new Kula-Chinook ridge. The Mendocino transform fault was, at this time, the lower boundary of the Chinook plate, and the Chinook-Farallon ridge the eastern boundary of the same plate. The Surveyor fracture zone represents relative motion between the Chinook and Farallon plates. Spreading along the newly formed Kula-Chinook ridge requires oblique spreading or strike-slip motion along the northern Emperor Trough.

Very slow spreading on the southern Emperor Trough probably continued until the Kula-Chinook ridge reached the Aleutian Trench. The Chinook plate then became part of the Pacific plate, probably at the time of anomalies 21 and 22 (~50 Ma).

Isochrons were drawn from M0 to the Hess Rise continuing the previous spreading rate from the Cenozoic lineations (Figure 4). The Rise must have been abandoned by a ridge jump to prevent its twin from being left on the Chinook plate. Deep Sea Drilling Project holes date the basal sediments on the Rise as Albian-Cenomanian. Thus the ridge probably abandoned the Rise in the Albian (113-97.5 Ma). Ridge abandonment was chosen to occur at 105 Ma for the isochron chart. To allow for spreading from the new ridge at 105 Ma to the Emperor Trough at 84 Ma and still give a sensible rate of spreading, the new ridge was located as close to the Hess Rise as possible.

Rea and Dixon (1983) did not treat the area immediately west of the Emperor Seamount Chain. For the isochron chart (Figure 4), the Japanese lineations were continued eastward to the Emperor Trough and northward to the Kurile Trench. The east west trending Cenozoic lineations that formed on the Kula-Chinook spreading center were continued westwards to the Emperor Trough and northwards to the Alentian Trench.

Mammerickx and Sharman (in press) presented an alternative model for the area treated by Rea and Dixon (1983) based on a re-evaluation of magnetic and bathymetric data. Their work unfortunately did not come to the attention of the authors in time to be included in the isochron chart. Their model is similar to that of Rea and Dixon (1983), but solves several problems. The difference between the two models hinges on the interpretation of the trend of the Surveyor Fracture Zone. Mammerickx and Sharman (in press) reprocessed the original magnetic and bathymetric data. They believe that the main part of the Surveyor is basically parallel to the Mendocino Fracture Zone. In addition, they argue that the western extension of the Surveyor that angles towards the Mendocino is not part of the Surveyor Fracture Zone proper. Also, the Mendocino Fracture Zone is not a simple linear feature in this area (Mammerickx, personal communication). Their proposition is a major simplification because it removes the necessity of an extra "Chinook" plate.

Mammerickx and Sharmann (in press) suggested that the "Chinook Plate" is simply a trapped piece of the old Farallon Plate and that the Emperor Trough is simply the site where the spreading center was abandoned at 84 Ma when the Pacific-Farallon ridge jumped eastward. This model does not change the ages from those presented in Figure 4 except in the immediate vicinity of the Emperor Trough. Mammerickx and Sharman (in press) also include a treatment of the area west of the Emperor Seamounts.

DEPTH AND AGE IN THE NORTH PACIFIC

In this section the gridded isochron chart and averaged depths are used in conjunction with charts of the sediment thickness to examine the relation between basement depth and age.

Determination of Basement Depth

SYNBAPS Bathymetry data (Van Wykhouse, 1973) which was averaged from five minute intervals to half degree intervals forms the basic data set. This interval retains the major bathymetric features (Figure 6). To determine the unloaded basement depth the SYNBAPS data was corrected for the oceanwide variation of the velocity of sound in sea water (Matthews, 1939) and the effects of sediment loading.

To correct for the sediment load, the sediment thickness chart of Ludwig and Houtz (1979) was gridded at half degree intervals. Unfortunately, high quality seismic data is scarce in the North Pacific, especially in the western area where Cretaceous basalt flows make the detection of basement difficult. The seismic data used by Ludwig and Houtz (1979) is variable in coverage and is concentrated around major port areas such as Hawaii and Guam.

Errors in the sediment thickness values given by Ludwig and Houtz (1979) may be largely due to the scarcity of data and the smoothing. Unfortunately, the margin of error cannot be quantified. It is likely that some of the errors are fairly random and are eliminated by treating the resulting depth versus age plot statistically. However, there is a possibility of systematic error in the western Pacific where the full thickness of the sediment column is largely unknown. Such an error will introduce a bias that will result in ocean basement depths that are shallower than they should be.

The "reverberant layer" (Houtz and Ludwig, 1979) was not included. Shipley et al., (1983) showed that the reverberations are at the dominant frequency of the seismic source, and they suggested that these reverberations do not actually represent layers of sediment.

The loading effect of the sediment was removed from the bathymetry using the method of Crough (1983). Crough (1983) found a linear relationship between the two-way travel time of sound through the sediment column and the traditional mass balance sediment correction. Crough (1983) based his study on drilling results from the Atlantic. We checked it for DSDP sites 462, 363, and 315 in the North Pacific and found that it was valid for this ocean as well as the Atlantic (Figure 7). We converted the data of Ludwig and Houtz (1979) into two-way travel time using the velocity/area relations given with the chart, and then multiplied the values by the slope of the empirical line (600 $\pm$m/sec). The resulting correction was added to the bathymetry to obtain the unloaded basement depths.

These basement depths were contoured at 500 m intervals (Figure 8). Because few areas contain thick sediments, Figure 8 shows almost all the same features shown by the uncorrected bathymetry (Figure 6). It is apparent from the corrected bathymetry that depth increases steadily from the East Pacific Rise until about the longitude of Hawaii (150°W). Between this longitude and the trenches the deep basins in the western North Pacific are dominated by a series of large swells, plateaus, and seamount chains.

The Relation Between Depth and Age

A plot of basement depth versus age for all the data in the North Pacific is presented in Figure 9. There is a general increase in depth with age for young ocean floor. For ocean floor greater than 80 Ma this increase is no longer clearly apparent.

Scatter in the data is a prominent feature of the distribution at all ages. Scatter increases dramatically at the age where the depth levels-off (about 80 Ma). The scatter can be attributed in part to errors in the age and sediment thickness data. An additional factor is variability in depth along a ridge axis. For example, the mid-ocean ridge in the Pacific is known to vary by $\pm$300 m around the mean value. However, most of the variation results from the inclusion of seamounts and trenches which account for the very shallow and very deep values.

The mean and second standard deviations were computed at one million year intervals with points weighted for the decrease in area of a half degree square with increasing latitude (Figure 10). These curves were superimposed on the raw data and compared with the subsidence curves computed for the 'plate' and 'simple boundary layer' models (Parsons and Sclater, 1977; Lister, 1977). Both model curves more or less match the observations for crust younger than about 75 Ma. For crust older than this, the mean lies well above both curves. In the case of the 'boundary layer' model, the predicted depth lies close to two standard deviations below the mean of the data.

For older sea floor the depth/age distribution is highly skwwed. This is illustrated clearly on Figure 10 where the distribution is obviously not symmetric about the mean. Because the mean and standard deviations are adequate only for a Gaussian distribution, they are a poor representation of the data. The distribution is biased towards the extreme high values. This bias results from the inclusion of seamounts which create only "highs" on the ocean floor. Ideally they should be removed from the data set.

However, this is very difficult because the point where the seamount blends into the surrounding ocean floor is a matter of conjecture. Also, the flexural moats around the seamounts have to be considered and these are even less well defined.

A possible way of dealing with this problem is a statistical approach which yields a representation of the distribution that is not overly influenced by a few very shallow depths. This approach has to highlight the "representative" behavior of the ocean floor. "Representative" in this case is defined as the relationship along which most of the values fall. It is clear that the majority of the points plot in the lower regions of the distribution, while the very high points are few and far between (Figures 9 and 10). "Representative" North Pacific ocean floor might be best defined by a line through the greatest concentration of points, or the mode.

The mode is defined in Figure 11 by a series of histograms taken at 20 my intervals across the distribution of depth versus age. The mode of each individual histogram is its peak. The line connecting these peaks represents the mode of the distribution. A mode can be recognized for all of the histograms. It is significantly lower than the mean because the shallow depths represent a fairly small percentage of the total number of points.

A clearer method of delineating the mode was suggested by Ross and Denham (personal communication). A histogram was constructed in 100 m intervals of depth at each 1 my age interval. The number of points that fell within each 1 my x 100 m bin was stored and the resulting grid was contoured. Point counts were weighted for the decrease in area of a half degree square with increasing latitude.

To choose the optimum contour value for defining the mode, different contours were tested and the percentage of points inside them calculated (Figure 12). 100% of the points lie within the first contour of Figure 12a which separates bins containing one or more points from those that contain none. The first contour of Figure 12b surrounds bins containing two or more points and the scatter has been reduced. Approximately 90% of all depths lie within ± 500 m of the mode for crust younger than 80 Ma. The scatter for older crust is still too large for a representative curve to be defined.

In Figures 12 c, d, and e, the first contour value has been raised successively by two with the object of achieving the narrowest band possible that is coherent at all ages. Figure 13e was selected in this manner as the most representative mode. The first contour of Figure 12e surrounds bins containing 8 or more points, or 56.06% of the total number of points. If the first contour value is increased further (Figure 12f) the mode loses coherency.

An examination of the successive plots with increasing first contour values indicates that for crust less than 80 Ma, more than 75% of the values lie within ± 300 m of the mode. For crust older than this, approximately the same number of values lie within ± 500 m (Figure 12c). Approximately 56% of all the values lie within ± 300 m of the mode (Figure 12e).

Comparison of Observations and Predictions

The plot of the chosen band about the mode (Figure 12e) is compared with the subsidence predicted by the 'plate' and 'boundary layer' models as calculated from equations given in Parsons and Sclater (1977) (Figure 13). Both predicted curves lie close to the mode band for crust less than 80 Ma. By 100 Ma, the square root of age relation of the 'boundary layer' model lies significantly below the band and the difference between the two increases with increasing age. The curve predicted by the 'plate model', with the exception of crust between 110 and 130 Ma and that greater than 160 Ma, lies within the mode band and along its deeper side. Except for these two regions, the curve predicted by the 'plate model' gives a reasonable representation of the data. Without implying any mechanism, it is clear from Figure 13 that the depth versus age curve predicted by the 'plate model' is a good representation of the mode of the data.

The relation between depth and age in the North Pacific is similar to that observed by Sclater and Wixon (in press) for the western North Atlantic (Figure 14). Again, like the Pacific, there are significant variations in the mode. In the western North Atlantic the shallowing between 100 and 120 Ma is created by the Bermuda Rise. Again, apart from this region, the subsidence curve predicted by the 'plate model' gives a reasonable prediction of the mode of the data.

Without implying any mechanism, it is clear from Figures 13 and 14 that the depth versus age cruve predicted by the 'plate model' is a reasonable representation of the flattening of mode of the data in both the North Pacific and western North Atlantic.

RESIDUAL DEPTH ANOMALIES AND CORRELATION WITH GEOID ANOMALIES

The residual depth is defined as the difference between the observed depth corrected for sediment load and the expected depth from some relation between depth and age. Clearly, to prevent any preconceived bias the depth/age relation should be empirically derived from the sum of all the data. However, such an empirical curve has not been developed and it is necessary to use theoretical models that have been fit to a limited number of topographic profiles.

We have shown that the depth predicted by the 'plate' model gives a good general match to the mode of the observations in the North Pacific. The depths computed by this model were subtracted from the basement depths to determine residual depths which were contoured at 500 m intervals (Figure 15). The difference between the curve predicted by the plate model and the mode of observations creates a slight ramp in the contour chart of residual depth. The ocean floor in the young eastern Pacific is generally deeper than the predicted curve, and the older ocean floor in the western Pacific is generally shallower.

Residual depth anomalies are perturbations in the expected relation between depth and age that may be created by a variety of mechanisms. Most of the striking anomalies are in the older western North Pacific. Most of the depths in the younger eastern North Pacific lie close to those predicted by the model. Wide regions that are slightly high and slightly low run parallel to the trend of the major fracture zones. The only prominent low in the eastern North Pacific is the area just west of the East Pacific Rise which has been recognized in other residual depth calculations (Cochran and Talwani, 1977; Schroeder, 1984). The anomaly is small (< 500 m) and is not considered further in this study.

Comparison with the Isochron Chart

The major residual depth anomalies are the prominent positive features of the Pacific west of and including Hawaii. Several basins between these features have slightly negative residual depth anomalies. A comparison of the residual depth chart of Figure 15 and the isochron chart of Figure 4 (Figure 16) shows that the positive residual depth anomalies correlate with rises of the mode at 120 and 160 Ma (Figure 13). The 120 Ma isochron runs through the Emperor seamounts, the western edge of the Hess Rise, the northern end of the Hawaiian swell, the Mid-Pacific Mountains, and the Line Islands. The predominance of positive features on crust about 120 Ma is responsible for the rise in the mode at that age. Most of the 140 Ma crust lies in the basins west of Hawaii and east of Japan, and most of the 160-170 Ma crust lies beneath the Marshall-Gilbert Islands, the Ontong-Java Plateau, the Mid-Pacific Mountains, and near the Marcus-Wake Island group. These features cause the rise in the mode on 160-170 Ma crust.

The rises in the mode shown on Figure 13 are clearly regionally coherent.

Comparison with Geoid and Heat Flow Data

It has been suggested that 500-1000 km wavelength residual depth anomalies in the oceans are associated with convection in the upper mantle. It is important to understand the nature of these features because it has been argued that such convection might be responsible for the flattening of the depth/age relationship.

All of the residual depth anomalies are associated with volcanics not directly related to normal sea floor spreading. Most of the western Pacific volcanism occurred in the middle and late Cretaceous (Rea and Vallier, 1983), with Eocene volcanism recorded in the Line and Marshall

Islands (Haggerty et al., 1982; Schlanger et al., 1981) and present day volcanism on the island of Hawaii. The volcanics probably indicate the presence of a convective plume beneath the plate at the time they were created. Volcanics by themselves are not evidence of any thermal anomaly in the plate today.

A topographic swell that has been uplifted by a thermal plume in the present or recent past and still has a thermal anomaly should have a corresponding distinctive geoid anomaly. Sandwell and Renkin (in press) examined the relationship between geoid height and topography for a number of swells and plateaus in the western Pacific. This relationship is useful for determining the mode of isostatic compensation for a specific plateau or swell (Haxby and Turcotte, 1978). A low ratio of geoid height to topography indicates that the topography is supported by thickened crust. A high geoid/topography ratio signifies deeper compensation which can be attributed to lithospheric thinning (Crough, 1978) and/or dynamic uplift from the rising limb of a convection cell (Parsons and Daly, 1983). An intermediate geoid/topography ratio suggests a combination of these two types of compensation (Sandwell and Renkin, in press).

The geoid data of Sandwell and Renkin (in preparation) was derived from SEASAT and GEOS-3 satellite altimeter data by Marsh et al. (1986). It was averaged from quarter degree intervals to half degree intervals, and a theoretical long wavelength geoid was removed with a Gaussian taper applied to coefficients from degrees 3 through 25. In their comparison with topography they used the sediment corrected SYNBAPS bathymetry of Figure 9.

A qualitative comparison of the geoid and residual depth charts for the western North Pacific can be seen in Figure 17. A high amplitude geoid anomaly over the Hawaiian Swell tapers-off with the topography into the southern Emperor Seamounts. A significant geoid swell also corresponds with the Line Islands, but all other the topographic anomalies in the western Pacific show almost no geoid signal.

Sandwell and Renkin (in press) selected ten features that they were able to divide into three groups on the basis of compensation. The Hawaiian Swell, with a high geoid/topography ratio, is most probably compensated by a thermal plume. The Line Islands, Midway Swell, and perhaps the Marcus-Wake Islands and the Hess Rise have intermediate geoid/topography ratios, suggesting perhaps a decaying thermal swell. However, the Marcus-Wake Islands may have this signal because of a scarp in the geoid to the north that may be unrelated to the islands, and the Hess Rise may appear this way because of its proximity to Midway. The Emperor Seamounts, Marshall-Gilbert Islands, Shatsky Rise, Mid-Pacific Mountains, and Ontong-Java Plateau all have low geoid/topography ratios and can all be explained as simple thickened crust.

On the basis of these results only the Hawaiian Swell can be considered to represent a present day convective plume. The Midway area, possibly the Marcus-Wake Swell and the Line Swell may represent decaying thermal plumes, although a plume in the process of reactivation is a possibility for the Line Swell. The rest of the features appear to be in isostatic equillibrium with the crust.

A thermal origin for the Hawaiian Swell is strongly supported by the existence of high heat flow on both the Hawaiian Swell and Bermuda Rise. Detrick et al. (in press) have shown that the shape, uplift, and subsidence histories of these two regions of anomalous depth can be accounted for by the lithosphere moving across a distributed heat source in the underlying upper mantle. The different absolute velocities of the Pacific and North American plates account for the different shapes of these features.

The geoid/topography relation for the Midway area agrees with the theory that this extension of the Hawaiian Swell formed when the plate passed over the Hawaiian hotspot 20-40 Ma and has since been subsiding according to a predicatable thermal cooling curve (Detrick and Crough, 1978; Menard and McNutt, 1982).

Heat flow data for other areas in the western Pacific is sparse and is concentrated in the old basins (Vacquier et al., 1966; Lister et al., in preparation). It appears to be of uniformly constant value as is to be expected of regions currently unaffected by a major thermal anomaly.

IMPLICATIONS FOR THERMAL MODELS OF THE LITHOSPHERE AND UPPER MANTLE

In this section we summarize our observations concerning depth and age and the relation between residual depth and geoid anomalies. The implication of these observations for two thermal models of the cooling lithosphere are examined. In addition, areas of anomalous depth, the processes they represent, and their bearing on the depth/age relation and thermal models of the lithosphere are discussed.

Summary of Observations

Seventy-five percent of all the $1/2 \times 1/2^{\circ}$ averages in the age range 0 - 80 Ma lie within 300 M of the modal value. In addition, the depth of the mode increases as the square root of time. It is also known that in well sedimented areas of the North Pacific, the heat flow decreases as one upon the square root of time (Sclater et al., 1981). It is generally accepted that simple cooling of the oceanic lithosphere explains both relations.

On older ocean floor the scatter in the depth data increases and the mode appears to flatten exponentially. However, there are large but coherent variations about this general flattening trend. Constructing a residual depth anomaly chart shows that these coherent variations in time are regionally correlatable in space. All occur on the old ocean floor of the western North Pacific.

Comparison of long wavelength regionally correlatable residual depth anomalies with geoid anomalies show that only the Hawaii Swell has a strong positive correlation and the Emperor Seamount chain has almost none at all. The Marcus-Wake, Line Island and Hess Rises have correlations similar to Midway. The Shatsky Rise, the Marshall Gilbert Swell, the Mid-Pacific Mountains, and the Ontong-Java Plateau show no correlation at all.

It is generally accepted that the excess volcanism and the Swell around Hawaii are associated with an upwelling mantle convection system. If this is the case, it is logical to interpret Midway as a much less active and the Emporer Seamount chain as a totally inactive portion of the same system. By analogy the Marcus-Wake, Hess Rise and Line Islands are interpreted as recently active (within the past 50 million years) swells.

Simple 'Boundary Layer' Cooling Model

The simple 'boundary layer' model (Turcotte and Oxburgh, 1967; Parker and Oldenburg, 1973) defines a rigid single layer lithosphere that thickens linearly with the square root of age as it cools by conduction (Figure 18a). This model predicts a relation between depth and the square root of age and heat flow and one upon the square root of age. Though heat flow observations are compatible with such a model to 120 Ma crust (Lister, 1977; Parsons and Sclater, 1977), the depth data agree with it only for crust less than 80 Ma. Beyond this age there is no evidence for continued subsidence at the predicted rate.

Heestand and Crough (1981) suggested that the flattening of old crust is caused by the perturbations of thermal plumes in the upper mantle that create mid-plate swells (Figure 18b). Schroeder (1984) postulated that a large number of such swells are needed in the Pacific to account for the widespread evidence for flattening of the depth/age relation in the older basins.

To check this explanation, we constructed the relation between depth and age along a flow line running between the Mendocino and Murray Fracture Zones (Figure 19) (though the Murray Fracture Zone probably should not be continued beyond 115 Ma). The mode of the depth has a general flattening trend close to that predicted by the plate model. The areas of depth shallower than expected lie on the northern end of the Hawaiian Swell (100-

120 Ma), the end of the Mid-Pacific Mountains (126–140 Ma), and the Marcus-Wake Island swell and the northern Marshall-Gilberts (160 Ma and greater). Note that the subsidence expected by the simple boundary layer model lies well below that observed. Even if mantle plumes are added to account for both the Midway and Marcus-Wake Swell, then the expected depth age profiles are too deep (Figure 20a). To construct the expected depth, we have used the geoid/depth correlation of Sandwell and Renkin (in press) to justify using a similar depth anomaly for the Marcus-Wake Swell as for Midway. Clearly only if this latter swell was a much larger phenomena could this model account for the observations.

Another observation difficult to explain by this modification of the simple boundary layer model is the large area north of 30° N and west of the Emperor Seamounts which contains no major depth anomalies except the Shatsky Rise. Most of the 130-150 Ma crust lies in these basins, as well as the Central Pacific Basin west of the Line Islands. Therefore, if the modification of 'boundary layer' model is valid, the mode at these ages would be expected to lie along the square root of age relation. This is not observed.

Clearly, some extra heat is needed to maintain the mode of the depths in these basins at a near constant value. It is not likely that plumes beneath the Hawaiian Swell and the Line Swell are providing this heat.

A caution needs to be entered at this point. The sediment thickness in the western North Pacific is not known with certainty. We have assumed that the basement picked by Ludwig and Houtz (1979) is correct. In the basins south of Japan there is evidence from Sono-buoy data that supports the thickness of sediment they inferred from seismic profiles. Further to the south, the evidence that they have correctly picked the top of the oceanic crust is much less convincing and, in fact, some very deep basement depths have been reported for localized areas in the Mariana basin (Whitman, 1985). Until this question is resolved unambiguously, it will not be certain that the 'boundary layer' model cannot account for the depth versus age relation on old crust. However, the reliable depth information south of Japan is evidence that the depths of thé deep basins do indeed flatten with increasing age.

'Plate' Model

The 'Plate' model of Parsons and McKenzie (1978) (Figure 21a) was constructed to provide an explanation for the flattening of the depth versus age relation in terms of thermal equilibrium between a lithosphere of constant thickness and the mantle. Parsons and McKenzie (1978) argued that in order for the lithosphere to reach thermal equilibrium within the age of existing ocean crust, heat must be transferred through the lithosphere convectively. The 'Plate' model defines a lithosphere with two layers: an upper rigid mechanical layer, and a lower viscous thermal layer that cools by conduction along with the upper layer when the plate is young. According to the model the viscous layer becomes unstable after a time and sustains small scale convection. The effect of convection in the thermal boundary layer is modelled by a constant temperature boundary condition at a fixed depth below the bottom of the rigid layer; hence, the name 'plate' model.

The 'plate' model predicts a general increase in depth with the square root of age until the effect of convection in the lower boundary is observed. After this time the depths should flatten exponentially to a constant value. This model gives a good general match to the exponential flattening in the depths in the western North Pacific as defined by the band around the mode in Figure 13. It does not explain the regionally correlatable residual depth anomalies.

It is relatively simple to modify this model to account for mid-ocean swells. For example, the numerical convection models of Parsons and Daly (1983) can be used to explain the Hawaiian Swell in terms of the 'plate' model. In their concept, the lower part of the lithosphere, the viscous thermal boundary layer, acts as the upper thermal boundary layer of mantle convection. Thus, a thermal plume in the upper mantle will penetrate through much of the lithosphere apparently heating it up fairly rapidly (Figure 21b). This will cause uplift and a geoid anomaly. Partial melting at the base of the mechanical layer will create volcanism. Evidence that excesve mid-plate volcanism formed the older seamount clusters and plateaus in the western Pacific suggests that they may be the remains of similar thermal plumes that operated beneath the lithosphere long ago.

To check this model we compared it with the subsidence along the flow line. In this case the general fit to the subsidence curve is excellent even under the assumption that the Marcus-Wake Island Swell is no more dramatic than that at Midway (Figure 20b).

Discussion

Clearly no very simple model will explain the observed subsidence on young crust, the flattening and the residual depth anomalies. The boundary layer model is inherently simpler inferring just boundary layer cooling and upper mantle plumes. However, it does not offer a satisfactory explanation of the observations. The thermo-mechanical 'plate' model is more complex, but it does offer a more satisfactory match to the observations. The data, as presently observed, favor some extra heat or other process that will flatten the lithosphere under old ocean floor. This process is in addition to those involved in the cooling of the lithosphere and thermal convection in the upper mantle.

CONCLUSIONS

The relation between depth and age on old ocean floor provides a major constraint on both cooling models of the lithosphere and convection in the upper mantle. Current observations require a process, in addition to those of cooling and major upwelling mantle convective plumes, to account for the flattening of the depths on old ocean floor. In the thermo-mechanical 'plate' model this process is thought to be the onsett of convection in the unstable thermal boundary layer.

Before the necessity of such a process can be unreservedly accepted, the sediment thickness in the western North Pacific needs to be rechecked. Addition of 500 m to 1 km to the deep basins in this area would significantly reduce the evidence which favored such a process. Both the thickness and the loading effect of the sediments in these areas need to be determined unambiguously.

The correlation between geoid height and residual depth anomalies presents a simple method for classifying the seamounts, plateaus and swells in the western North Pacific (Sandwell and Renkin, in press). It is proposed that some of these features represent different stages in the cooling history of an upper mantle plume that has reset the thermal structure of the cooling lithosphere. Heat flow measurements both on and off the Marcus-Wake and Line Island Swells are needed to check this suggestion. Further, the subsidence of guyots on these features which show a positive geoid/depth correlation need to be compared with similar features that show no such correlation.

The overall subsidence of the ocean floor can be accounted for by the cooling of a thermo-mechanical boundary layer perturbed by upwelling convective plumes in the upper mantle. These plumes may be responsible for much of the secondary volcanism that gives rise to the seamount chains, plateaus and swells in the western North Pacific. Thus, it is possible that a single process observed at different times in its history may be responsible for many of the depth anomalies in the western North Pacific.

BIBLIOGRAPHY

Anderson, R. N., and E. E. Davis, A topographic interpretation of the Mathematician Ridge, Clipperton Ridge, East Pacific Rise system, Nature, 241, 191-193, 1973.

Atwater, T., and H. W. Menard, Magnetic lineations in the northeast Pacific, Earth Planet. Sci. Lett., 7, 445-450, 1970.

Cande, S. C., R. L. Larson, W. C. Pitman, X. Golovchenko, J. F. Dewey, W. F. Haxby, and J. L. LaBrecque, Magnetic Lineation Map of the World, (in press).

Cochran, J. R., and M. Talwani, Free-air gravity anomalies in the world's oceans and their relationship to residual elevation, Geophys. J. R. Astron. Soc., 50, 495-552, 1977.

Crough, S. T., Thermal origin of mid-plate hot-spot swells, Geophys. J. R. Astron. Soc., 55, 451-469, 1978.

Crough, S. T., The correction for sediment loading on the sea floor, J. Geophys. Res., 88, 6449-6454, 1983.

Crough, S. T., and R. D. Jarrard, The Marquesas-Line swell, J. Geophys. Res., 86, 11763-11771, 1981.

Davis, E. E., and C. R. B. Lister, Fundamentals of ridge crest topography, Earth Planet. Sci. Lett., 21, 405-413, 1974.

Detrick, R. S., An analysis of geoid anomalies across the Mendocino Fracture Zone: Implications for thermal models of the lithosphere, J. Geophys Res., 86, 11,751-11,762, 1981.

Detrick, R. S., and S. T. Crough, Island subsidence, hot spots, and lithospheric thinning, J. Geophys. Res., 83, 1236-1244, 1978.

Detrick, R.S., R. P. Von Herzen, B. Parsons, D. Sandwell, and M. Dougherty, Heat flow observations on the Bermuda Rise and thermal models of mid-plate swells, J. Geophys. Res., submitted, 1985.

Farrar, E., and J. M. Dixon, Early Tertiary rupture of the Pacific Plate: 1700km of dextral offset along the Emperor Trough - Line Islands lineament, Earth Planet. Sci. Lett., 53, 307-322, 1981.

Gordon, R. G., Paleomagnetic test of the Emperor fracture zone hypothesis, Geophys. Res. Lett., 9, 1283-1286, 1982.

Haggerty, J. A., S. O. Schlanger, and I. Premoli-Silva, Late Cretaceous and Eocene volcanism in the southern Line Islands and implications for hotspot theory, Geology, 10, 433-437, 1982.

Haxby, W. F., and D. L. Turcotte, On isostatic geoid anomalies, J. Geophys. Res., 83, 5473-5478, 1978.

Heestand, R. L., and S. T. Crough, The effect of hotspots on the oceanic age-depth relation, J. Geophys. res., 86, 6107-6114, 1981.

Hilde, T. W. C., S. Uyeda, and L. Kroenke, Evolution of the western Pacific and its margin, in Present State of Plate Tectonics, edited by J. Bonnin and R. S. Dietz, Tectonophysics, 38(1-2), 145-165, 1977.

Houtz, R. E., and W. J. Ludwig, Distribution of reverberant subbottom layers in the southwest Pacific basin, J. Geophys. Res., 84, 3497-3504, 1979.

Jackson, E. D., and S. O. Schlanger, Regional synthesis, Line Islands chain, Tuamotu Island chain, and Manihiki Plateau, Central Pacific Ocean, in Initial Reports of the Deep sea Drilling Project, Volume 33, edited by S. O. Schlanger, E. D. Jackson, et al., pp. 915-927, U.S. Government Printing Office, Wasington, D.C., 1976.

Kent, D. V., and F. M. Gradstein, A Jurassic to Recent Chronology, in The Western Atlantic region, Volume M of the geology of North America, edited by B. E. Tucholke and P. R. Vogt, Geological Society of America, Boulder, Colorado (in press).

Klitgord, K. D., and J. Mammerickx, Northern East Pacific Rise: magnetic anomaly and bathymetric framework, J. Geophys. Res., 87, 6725-6750, 1982.

Langseth, M. S., X. LePichon, and M. Ewing, Crustal structure of mid-ocean ridges, 5. heat flow through the Atlantic ocean and convection currents, J. Geophys. Res., 71, 5321-5355, 1966.

Larson, R. L., Late Jurassic and early Cretaceous evolution of the western central Pacific ocean, J. Geomag. Geoelectr., 28, 219-236, 1976.

Larson, R. L., W. C. Pitman, X. Golovchenko, S. C. Cande, J. F. Dewey, W. F. Haxby, and J. L. LaBrecque, The Bedrock Geology of the World, W. H. Freeman and Company, Inc. New York, New York, 1985.

Lee, W. H. K., and S. Uyeda, Review of heat flow data, in Terrsetrial Heat Flow, Geophysical Monograph 8, pp. 87-190, American Geophysical Union, Washington, D.C., 1965.

Lister, C. R. B., On the thermal balance of a mid-ocean ridge, Geophys. J. R. Astron. Soc., 26, 515-535, 1972.

Lister, C. R. B., Estimators for heat flow and deep rock properties based on boundary layer theory, In: A. M. Jessop, ed., Heat Flow and Geodynamics, Tectonophysics, 41, 157-171, 1977.

Lister, C. R. B., E. E. Davis, and J. G. Sclater, Mariana Basin heat flow, (perpetually in preparation).

Ludwig, W. J., and R. E. Houtz, Isopach Map of Sediments in the Pacific Ocean Basin and Marginal Sea Basins, American Association of Petroleum Geologists, Tulsa, Oklahoma, 1979.

Mammerickx, J., and D. Sandwell, Birth and evolution of long distance spreading center jumps (abstract), EOS Trans. AGU, 66(18), 356, 1985.

Mammerickx, J., and G. Sharman, Evolution of the North Pacific during the Cretaceous quiet period, (in press).

Mammerickx, J., and S. M. Smith, Bathymetry of the Western North Pacific, Geological Society of America map Chart Series, (in press).

Marsh, J. G., A. C. Brenner, B. D. Becklet, and T. V. Martin, Global mean sea surface based on the SEASAT altimeter data, J. Geophys. Res., submitted, 1986.

Matthews, D. J., Tables of the Velocity of Sound in Pure Water and Sea Water for use in Echo Sounding and Sound Ranging, Hydrographic Department, The Admiralty, London, 1939.

McKenzie, D. P., Some remarks on heat flow and gravity anomalies, J. Geophys. Res., 72, 6261-6273, 1967.

McKenzie, D. P., J. M. Roberts, and N. O. Weiss, Convection in the earth's mantle: towards a numerical simulation, Journal of Fluid Mechanics, 62, 465-538, 1974.

McKenzie, D. P., A. Watts, B. Parsons, and M. Roufosse, Planform of mantle convection beneath the Pacific Ocean, Nature, 288, 442-446, 1980.

Menard, H. W., and L. M. Dorman, Dependence of depth anomalies upon latitude and plate motion, J. Geophys. Res., 82, 5329-5335.

Menard, H. W., and Marcia McNutt, Evidence for and consequences of thermal rejuvenation, J. Geophys. Res., 87, 8570-8580, 1982.

Parker, R. L., and D. W. Oldenburg, Thermal model of ocean ridges, Nature Phys. Sci., 242, 137-139, 1973.

Parsons, B., and S. Daly, The relationship between surface topography, gravity anomalies, and temperature structure of convection, J. Geophys. Res., 88, 1129-1144, 1983.

Parsons, B., and D. McKenzie, Mantle convection and the thermal structure of the plates, J. Geophys. Res., 83, 4485-4496, 1978.

Parsons, B., and J. G. Sclater, An analysis of the variation of ocean floor bathymetry and heat flow with age, J. Geophys. Res., 82, 803-827, 1977.

Rea, D. K., and J. M. Dixon, Late Cretaceous and Paleogene tectonic evolution of the North Pacific ocean, Earth and Planet. Sci. Lett., 65, 145-166, 1983.

Rea, D. K., and T. L. Vallier, Two Cretaceous volcanic episodes in the western Pacific Ocean, Geological Society of America Bulletin, 94, 1430-1437, 1983.

Roufosse, M., B. Parsons, D. McKenzie, and A. B. Watts, Geoid and depth anomalies in the Indian Ocean [abstr.], EOS, Trans. AGU, 62, 389, 1981.

Sager, W. W., and B. H. Keating, Paleomagnetism of the Line Islands seamounts: evidence for late Cretaceous and early Tertiary volcanism, J. Geophys. Res., 89, 11335-11151, 1984.

Sandwell, D. T., and M. L. Renkin, Compensation of swells and plateaus in the North Pacific: no direct evidence for mantle convection, (in preparation).

Schlanger, S. O., J. F. Campbell, J. A. Haggerty, and I. Premoli-Silva, Cretaceous volcanism and Eocene failed atolls in the Radak chain: implications for the geological history of the Marshall Islands (abstract), EOS Trans. AGU, 62(45), 1075, 1981.

Schlanger, S. O., M. O. Garcia, B. H. Keating, J. J. Naughton, W. W. Sager, J. A. Haggerty, J. A. Philpotts, and R. A. Duncan, Geology and geochronology of the Line Islands, J. Geophys. Res., 89, 11261-11272, 1984.

Schroeder, W., The empirical age-depth relation and depth anomalies in the Pacific ocean basin, J. Geophys. Res., 89, 9873-9883, 1984.

Sclater, J. G., R. N. Anderson, and M. L. Bell, Elevation of ridges and evolution of the central eastern Pacific, J. Geophys. Res, 76, 7888-7915, 1971.

Sclater, J. G., J. Crowe, and R. N. Anderson, On the reliability of oceanic heat flow averages, J. Geophys. Res., 81, 2997-3006, 1976.

Sclater, J. G., and J. Francheteau, The implications of terrestrial heat flow observations on current tectonic and geochemical models of the crust and upper mantle of the earth, Geophys. J. R. Astron. Soc., 20, 509-542, 1970.

Sclater, J. G., C. Jaupart, and D. Galson, The heat flow through oceanic and continental crust and the heat loss of the earth, Reviews of Geophysics and Space physics, 18, 269-311, 1980.

Sclater, J. G., L. A. Lawver, and B. Parsons, Comparison of long-wavelength residual elevation and free air gravity anomalies in the North Atlantic and possible implications for the thickness of the lithospheric plate, J. Geophys. Res., 80, 1031-1052, 1975.

Sclater, J. G., and L. Wixon, The relationship between depth and age and heat flow and age in the Western North Atlantic, in The Western Atlantic region, Volume M of the Geology of North America, edited by B. E. Tucholke and P. R. Vogt, Geological Society of America, Boulder, Colorado (in press).

Shipley, T. H., J. M. Whitman, F. K. Duennebier, and L. D. Petersen, Seismic stratigraphy and sedimentation history of the East Mariana Basin, western Pacific, Earth and Planet. Sci. Lett., 64, 257-275, 1983.

Sleep, N. H., Sensitivity of heat flow and gravity to the mechanism of sea floor spreading, J. Geophys. Res., 74, 542-549, 1969.

Tamaki, K., M. Joshima, and R. L. Larson, Remanent Early Cretaceous spreading center in the central Pacific basin, J. Geophys. Res., 84, 4501-4510, 1978.

Turcotte, D. L., and E. R. Oxburgh, Finite amplitude convection cells and continental drift, J. Fluid Mechanics, 28, 29-42, 1967.

Vacquier, V., S. Uyeda, M. Yasui, J. G. Sclater, C. Corry, and T. Watanabe, Studies of the thermal state of the earth, 21, Heat flow measurements in the northwestern Pacific, Tokyo University Earthquake Research Institute Bulletin, 44, 1519-1535, 1966.

Vallier, T. L., W. E. Dean, D. K. Rea, and J. Thiede, Geologic evolution of Hess Rise, central North Pacific Ocean, Geological Society of America Bulletin, 94, 1289-1307, 1983.

Van Wykhouse, R., SYNBAPS (Synthetic Bathymetric Profiling Systems), Technical Report TR-233, Naval Oceanographic Office, Washington, D.C., 1973.

Vogt, P. R., and N. A. Ostenso, Steady state crustal spreading, Nature, 215, 811-817

Watts, A. B., Gravity and bathymetry in the central Pacific Ocean, J. Geophys Res., 81, 1533-1553, 1976.

Watts, A. B., D. P. McKenzie, B. Parsons, and M. Roufosse, The relationship between gravity and bathymetry in the Pacific Ocean, Geophys. J. R. Astron. Soc., 83, 263-298, 1985.

Whitman, J. M., Mariana Basin: thick sediments and deep crust (abstract), EOS Trans. AGU, 66(18), 374, 1985.

Winterer, E. L., Anomalies in the tectonic evolution of the Pacific, in The Geophysics of the Pacific Ocean Basin and its Margin, Geophysical Monograph Series, 19, pp. 269-278, American Geophysical Union, 1976.

Winterer, E. L., Bathymetry and Regional tectonic setting of the Line Islands chain, in Initial Reports of the Deep Sea Drilling Project, Volume 33, edited by S. O. Sclanger, E. D. Jackson, et al., pp. 731-747, U.S. Government Printing Office, Washington, D.C., 1976.

Winterer, E. L., and J. Mammerickx, Bathymetry of the Line Islands region (map), in Initial Reports of the Deep Sea Drilling Project, Volume 33, edited by S. O. Sclanger, E. D. Jackson, et al., Plate 1, U.S. Government Printing Office, Washington, D.C., 1976.

Shipley, T. H., J. M. Whitman, F. K. Duennebier, and L. D. Petersen, Seismic stratigraphy and sedimentation history of the East Mariana Basin, western Pacific, Earth and Planet. Sci. Lett., 64, 257-275, 1983.

Sleep, N. H., Sensitivity of heat flow and gravity to the mechanism of sea floor spreading, J. Geophys. Res., 74, 542-549, 1969.

Tamaki, K., M. Joshima, and R. L. Larson, Remanent Early Cretaceous spreading center in the central Pacific basin, J. Geophys. Res., 84, 4501-4510, 1978.

Turcotte, D. L., and E. R. Oxburgh, Finite amplitude convection cells and continental drift, J. Fluid Mechanics, 28, 29-42, 1967.

Vacquier, V., S. Uyeda, M. Yasui, J. G. Sclater, C. Corry, and T. Watanabe, Studies of the thermal state of the earth, 21, Heat flow measurements in the northwestern Pacific, Tokyo University Earthquake Research Institute Bulletin, 44, 1519-1535, 1966.

Vallier, T. L., W. E. Dean, D. K. Rea, and J. Thiede, Geologic evolution of Hess Rise, central North Pacific Ocean, Geological Society of America Bulletin, 94, 1289-1307, 1983.

Van Wykhouse, R., SYNBAPS (Synthetic Bathymetric Profiling Systems), Technical Report TR-233, Naval Oceanographic Office, Washington, D.C., 1973.

Vogt, P. R., and N. A. Ostenso, Steady state crustal spreading, Nature, 215, 811-817

Watts, A. B., Gravity and bathymetry in the central Pacific Ocean, J. Geophys Res., 81, 1533-1553, 1976.

Watts, A. B., D. P. McKenzie, B. Parsons, and M. Roufosse, The relationship between gravity and bathymetry in the Pacific Ocean, Geophys. J. R. Astron. Soc., 83, 263-298, 1985.

Whitman, J. M., Mariana Basin: thick sediments and deep crust (abstract), EOS Trans. AGU, 66(18), 374, 1985.

Winterer, E. L., Anomalies in the tectonic evolution of the Pacific, in The Geophysics of the Pacific Ocean Basin and its Margin, Geophysical Monograph Series, 19, pp. 269-278, American Geophysical Union, 1976.

Winterer, E. L., Bathymetry and Regional tectonic setting of the Line Islands chain, in Initial Reports of the Deep Sea Drilling Project, Volume 33, edited by S. O. Sclanger, E. D. Jackson, et al., pp. 731-747, U.S. Government Printing Office, Washington, D.C., 1976.

Winterer, E. L., and J. Mammerickx, Bathymetry of the Line Islands region (map), in Initial Reports of the Deep Sea Drilling Project, Volume 33, edited by S. O. Sclanger, E. D. Jackson, et al., Plate 1, U.S. Government Printing Office, Washington, D.C., 1976.

Winterer, E. L., and C. V. Metzler, Origin and subsidence of guyots in Mid-Pacific Mountains, J. Geophys. Res., 89, 9969-9979, 1984.

Woods, M. T., and G. F. Davies, Late Cretaceous genesis of the Kula plate, Earth and Planet. Sci. Lett., 58, 161-166, 1982.

FIGURE CAPTIONS

Fig. 1. Magnetic lineations for the North Pacific from Cande et al. (in press) "Quiet zone" areas labled A, B, and C were assigned ages based on published tectonic reconstructions.

Fig. 2. Tectonic history of quiet zone A of fig. 1, based on the reconstruction of Hilde et al. (1977) relative to a fixed Pacific plate. Spreading ridges are represented by double lines, fracture zones by single lines, and the proposed isochrons on the Pacific plate by dashed lines. The Izanagi-Farallon-Phoenix triple junction (a) opened into three triple junctions about 174 Ma with the Pacific plate forming in the center (b). Between 165 and 160 Ma, (c and d) a segment of the Pacific-Izanagi ridge jumped to the northwest, taking the triple junction with it. This created the offset across the fracture zone cutting the ridge. By 160 Ma, the Pacific-Farallon-Phoenix plates met at a fault-fault-ridge triple junction.

Fig. 3. Quiet zone B of fig. 1, with 5 Ma isochrons based on the magnetic lineations of Cande et al. (in press) and the reconstruction of Larson (1976). Lettered areas between pairs of fracture zones are referred to in the text.

Fig. 4. Isochron chart for the North Pacific based on the magnetic lineation compilation of Cande et al. (in press) and the tectonic histories of Hilde et al. (1977), Larson (1976), and Rea and Dixon (1983). Contour interval is 5 My.

Fig. 5. Tectonic reconstruction of quiet zone C (Fig. 1) from Rea and Dixon (1983) relative to a fixed Pacific plate. Spreading ridges are represented by double lines and fracture zones by single lines. As the triple junction between the Pacific, Farallon, and Izanagi plates moved north into the quiet zone, slow spreading on the Pacific-Farallon ridge formed the Hess Rise about 110 to 100 Ma. About anomaly 34 time (84 Ma), the old triple junction was probably terminated and a new one opened further east, creating the Chinook plate. This required oblique separation across the Mendocino transform. Slow spreading continued on the Emperor Trough until about 50 Ma, when the new triple junction was terminated and the Chinook plate became part of the Pacific plate (modified from Rea and Dixon, 1983).

Fig. 6. SYNBAPS bathymetry with important features labled. The data has been averaged from five minute intervals to half degree intervals, and corrected for variations in the velocity of sound in sea water. The chart was contoured by computer in 500m intervals.

Fig. 7. The empirical relationship of Crough (1983) between the standard mass balance sediment correction and the two way travel time of seismic waves through the sediment column. Data from the North Pacific has been included. The linearity of this relationship is due to the self-cancellation of increases in velocity and density with depth.

Fig. 8. Half degree averaged SYNBAPS bathymetry corrected for the effects of sediment loading. Contour interval is 500m. This chart was contoured by computer.

Fig. 9. Depth versus age in the North Pacific, with points taken at half degree intervals. The histogram shows the total number of points in a given lmy interval.

Fig. 10. Depth versus age in the North Pacific with the mean and second standard deviations. Because of the skewness of the distribution, the mean and standard deviations are not meaningful parameters. For reference also are the 'plate' model and 'square root of age' curves calculated from equations given in Parsons and Sclater (1977).

Fig. 11. Histograms taken at 20 Ma intervals along the depth versus age distribution for the North Pacific.

Fig. 12. Contours surrounding the mode of the depth versus age distribution. A histogram was constructed in 100m intervals of depth at each 1 My age interval. The number of points that fell in each 1 My x 100m bin was stored, and the resulting grid was contoured. Point counts were weighted for the decrease in area of a half degree square with increasing latitude. (a) shows the zero contour, which surrounds 100% of the points. (b)-(f) show the results of increasing the first contour value successively (with various contour intervals). The contour that formed the narrowest band coherent over all ages (e) was selected as the most representative mode curve. The first contour of (e) surrounds boxes containing 8 or more points, or 56.06% of the total number of points. If the first contour is raised further (f), the mode loses coherency.

Fig. 13. The mode contour selected as most representative. 100m x 1 My boxes within the first contour contain 8 or more points, or 56.06% of the total.

Fig. 14. Depth versus age in the western North Atlantic. Data from Sclater and Wixon (in press) have been replotted at the scale of the North Pacific plots. The first mode contour (b) encloses 51.4% of the points.

Fig. 15. A chart of "residual depth" in the North Pacific. It shows the difference between basement depth at any point and the depth predicted for that age by the 'plate' model (Parsons and Sclater, 1977). This chart was contoured by computer in 500m intervals.

Fig. 16. "Residual depth" in the North Pacific with 100, 120, 140, and 160 Ma isochrons. Contour interval is 1000m. Most of the 120 and 160 Ma crust lies beneath the positive features while most of the 140 Ma crust lies in the basins. This correspondence is responsible for the rise in the mode around 120 Ma, the low at 140 Ma, and the rise again at 160 Ma.

Fig. 17. Smoothed geoid (dashed) and residual depth (solid) for the western North Pacific. The geoid data and the residual depths have been smoothed by a Gaussian filter to remove wavelengths shorter than 600km. Contour interval for the geoid is 3m, contour interval for the residual depths is 1000m.

Fig. 18a. The 'boundary layer' model of the lithosphere. Distance from ridge crest is roughly equivalent to age. T_m is the temperature of the mantle and the dashed lines are isotherms. The lithosphere increases in thickness with age and the bottom boundary is an isotherm. (from Parker and Oldenburg, 1973).

Fig. 18b. Interaction of a 'boundary layer' lithosphere with a mid-plate hot-spot. From the ridge to the hot-spot the lithosphere thickens and subsides by cooling. At the hot-spot, extra heat drives the isotherms upwards, thins the lithosphere and causes uplift. Beyond the hot-spot, the lithosphere cools rapidly because it is thin and thus subsides as younger lithosphere at the same depth, rather than as normal lithosphere of the same age (dashed line). (from Crough, 1978).

Fig. 19. Depth versus age along a "flow line". The area was selected to include crust which formed between the Mendocino and Murray Fracture Zones (a). In this line, all the 120 Ma crust lies on the northern end of the Hawaiian Swell, the 145 Ma crust in the Kalaniopu basin, and the 160-170 Ma crust on the Marshall-Gilbert Islands and the Marcus-Wake Island group. Fluctuations of the outer mode contour (c), which surrounds 63.24% of the points, are directly related to these features.

Fig. 20a. Subsidence expected from the simple boundary layer cooling model modified by the effect of upper mantle plumes. The plume under the Marcus-Wake Islands is assumed to be of the same magnitude as that under Midway Island.

Fig. 20b. Subsidence expected from the thermo-mechanical 'plate' model modified by the effect of similar size upper mantle plumes under the Marcus-Wake Island chain and Midway Island.

Fig. 21a. The 'plate' model of the lithosphere. This schematic diagram shows the division of the plate into rigid and viscous regions and the occurrence of an instability in the bottom viscous part of the plate. (modified from Parsons and McKenzie, 1978).

Fig. 21b. Interaction of a 'plate' model lithosphere with convection in the upper mantle. Solid lines represent isotherms. The horizontally averaged temperature structure is shown on the right. This is roughly the temperature structure that might be expected beneath features such as the Bermuda Rise. (from Parsons and Daly, 1983).

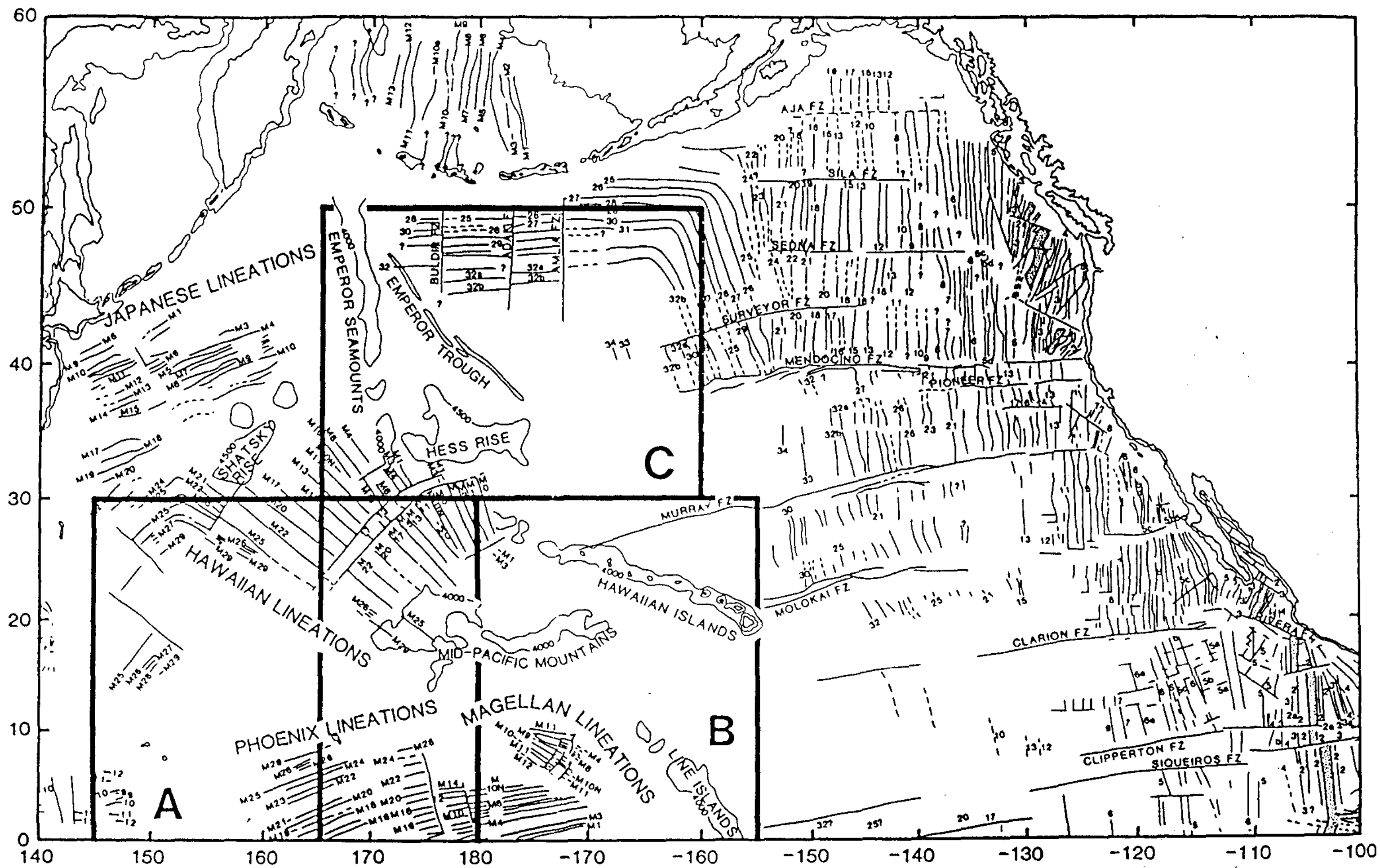

JAPANESE LINEATIONS
EMPEROR SEAMOUNTS
EMPEROR TROUGH
BULDIR FZ
AMLIA FZ
HESS RISE
SHATSKY RISE
HAWAIIAN LINEATIONS
HAWAIIAN ISLANDS
MURRAY FZ
MOLOKAI FZ
MID-PACIFIC MOUNTAINS
PHOENIX LINEATIONS
MAGELLAN LINEATIONS
LINE ISLANDS
AJA FZ
SILA FZ
SEDNA FZ
SURVEYOR FZ
MENDOCINO FZ
PIONEER FZ
CLARION FZ
CLIPPERTON FZ
SIQUEIROS FZ
A
B
C
60
50
40
30
20
10
0
140
150
160
170
180
−170
−160
−150
−140
−130
−120
−110
−100

Fig 1

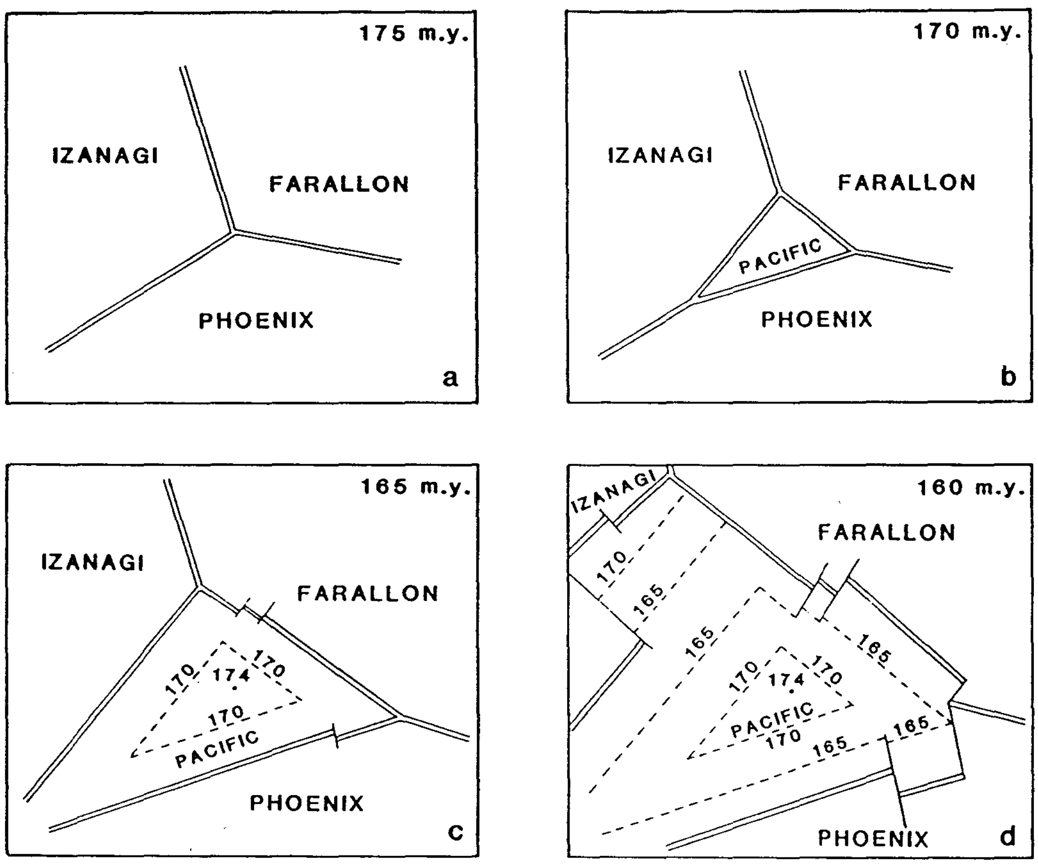
175 m.y.
IZANAGI
FARALLON
PHOENIX
a
170 m.y.
IZANAGI
FARALLON
PACIFIC
PHOENIX
b
165 m.y.
IZANAGI
FARALLON
170
174
170
170
PACIFIC
PHOENIX
c
160 m.y.
IZANAGI
FARALLON
170
165
165
165
170
174
170
PACIFIC
170
165
165
PHOENIX
d

fig 2

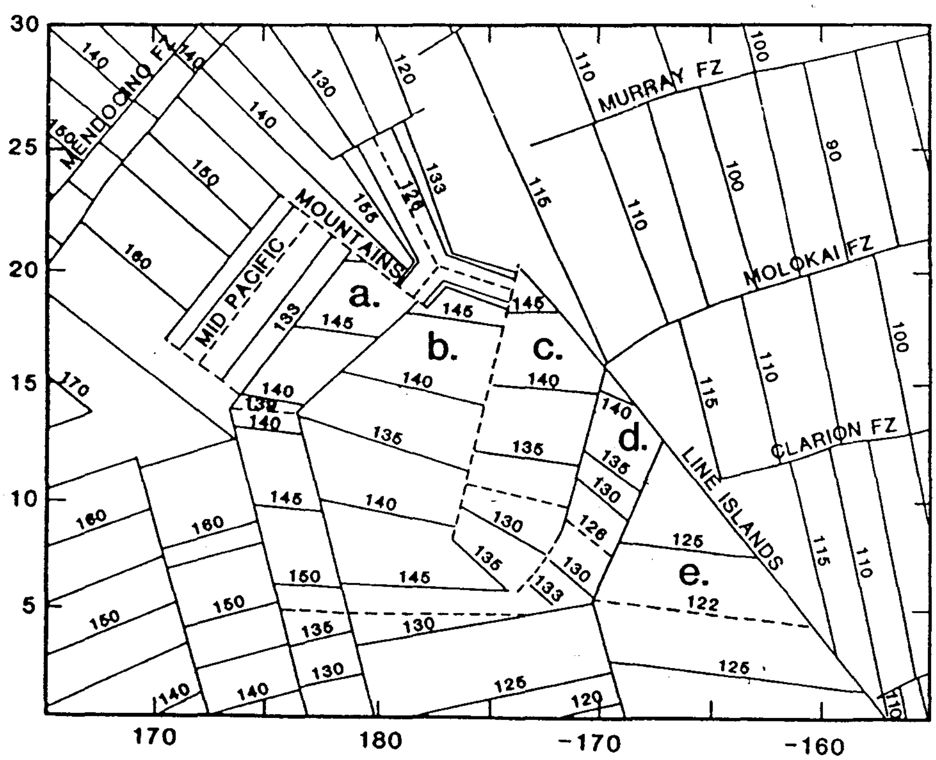

MENDOCINO FZ
MID PACIFIC MOUNTAINS
MURRAY FZ
MOLOKAI FZ
CLARION FZ
LINE ISLANDS
a.
b.
c.
d.
e.
30
25
20
15
10
5
170
180
-170
-160

fig 3

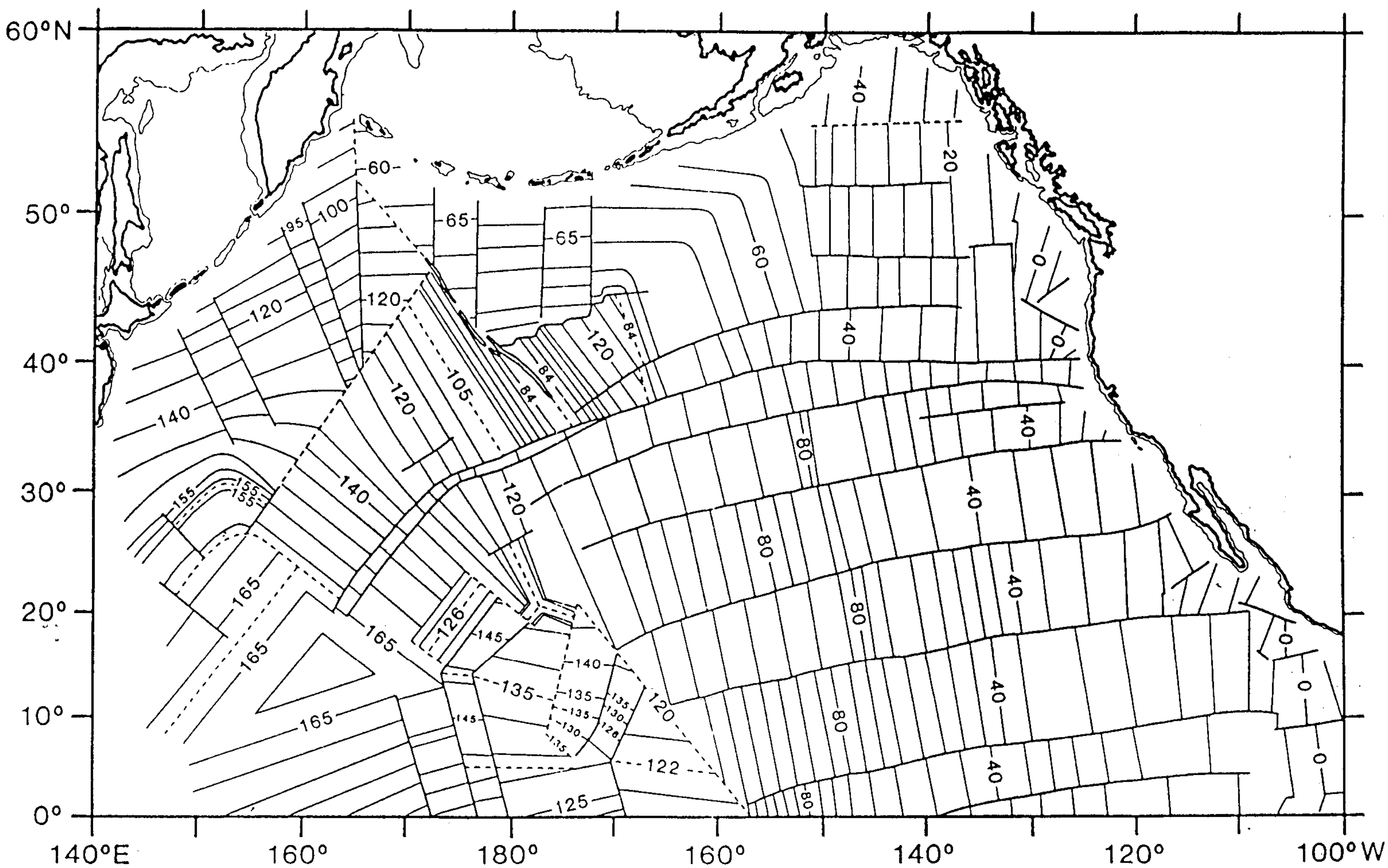

fig 4

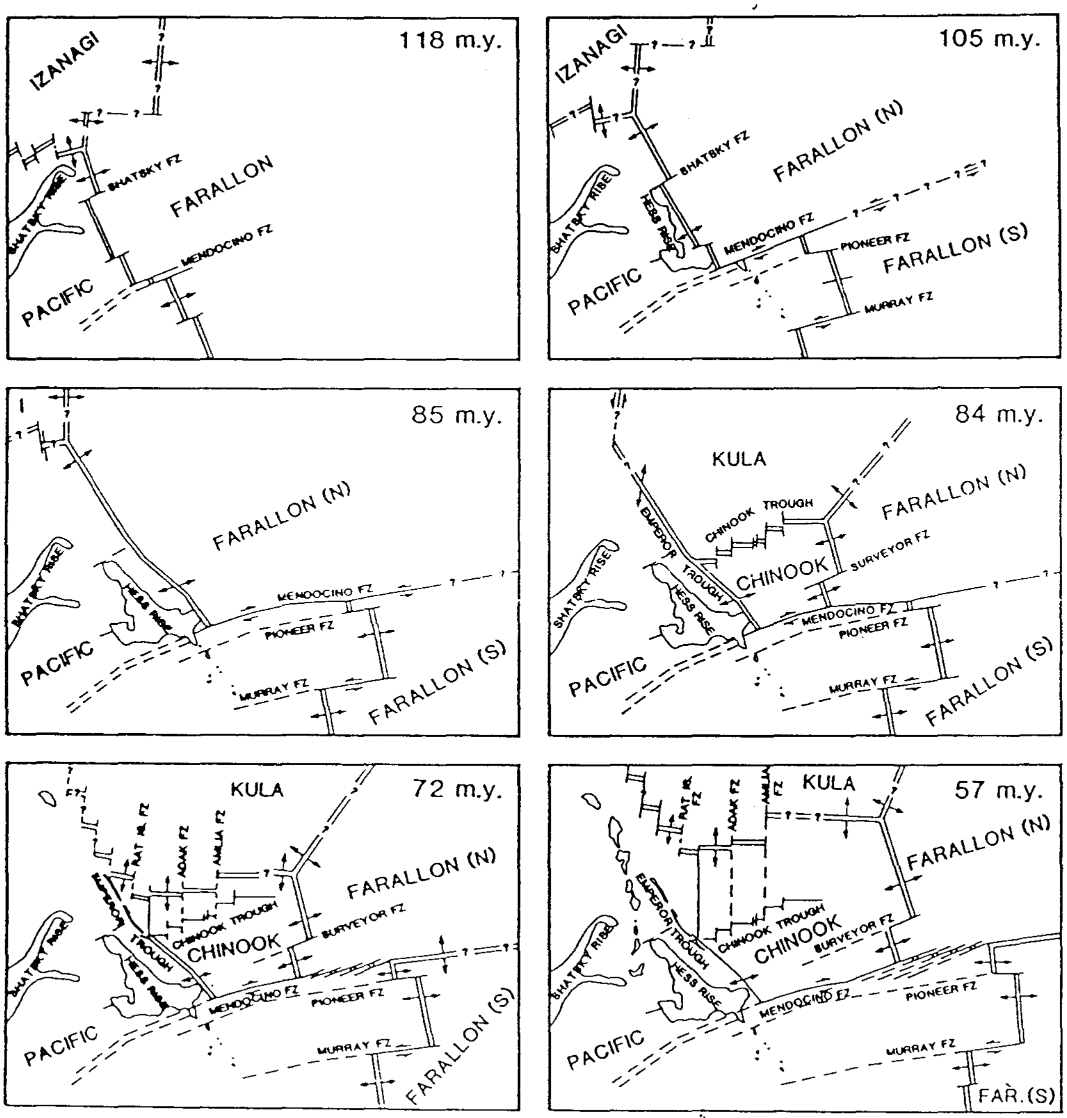
118 m.y.
IZANAGI
SHATSKY FZ
FARALLON
SHATSKY RISE
MENDOCINO FZ
PACIFIC
105 m.y.
FARALLON (N)
HESS RISE
PIONEER FZ
FARALLON (S)
MURRAY FZ
85 m.y.
84 m.y.
KULA
CHINOOK TROUGH
SURVEYOR FZ
EMPEROR TROUGH
CHINOOK
72 m.y.
RAT FZ
ADAK FZ
AMLIA FZ
57 m.y.
FAR.(S)

Fig. 5.

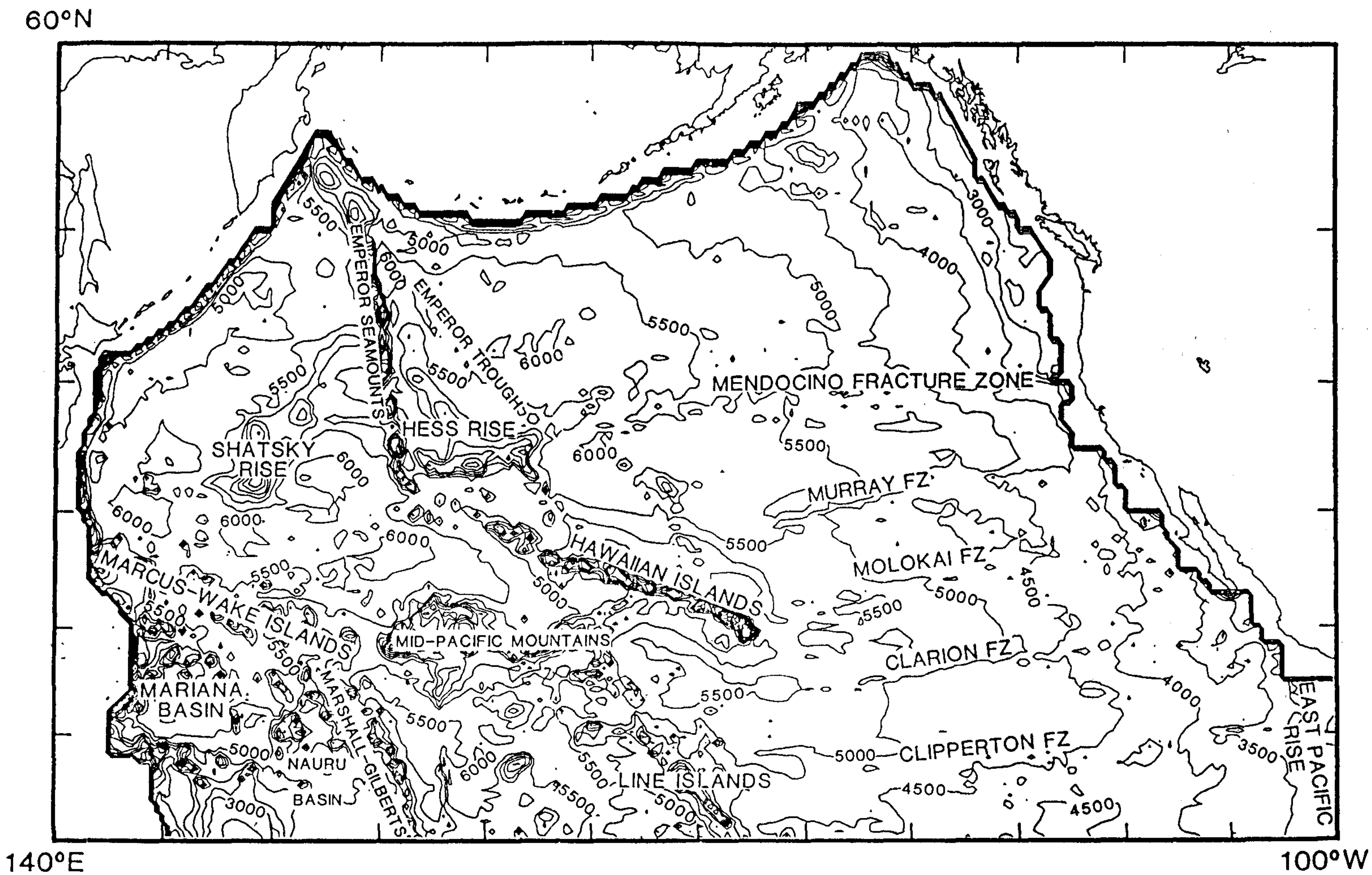
60°N
140°E
100°W
EMPEROR SEAMOUNTS
EMPEROR TROUGH
HESS RISE
SHATSKY RISE
MENDOCINO FRACTURE ZONE
MURRAY FZ
MOLOKAI FZ
CLARION FZ
CLIPPERTON FZ
HAWAIIAN ISLANDS
MARCUS-WAKE ISLANDS
MID-PACIFIC MOUNTAINS
MARIANA BASIN
MARSHALL-GILBERTS
NAURU BASIN
LINE ISLANDS
EAST PACIFIC RISE
3000
3500
4000
4500
5000
5500
6000

fig 6

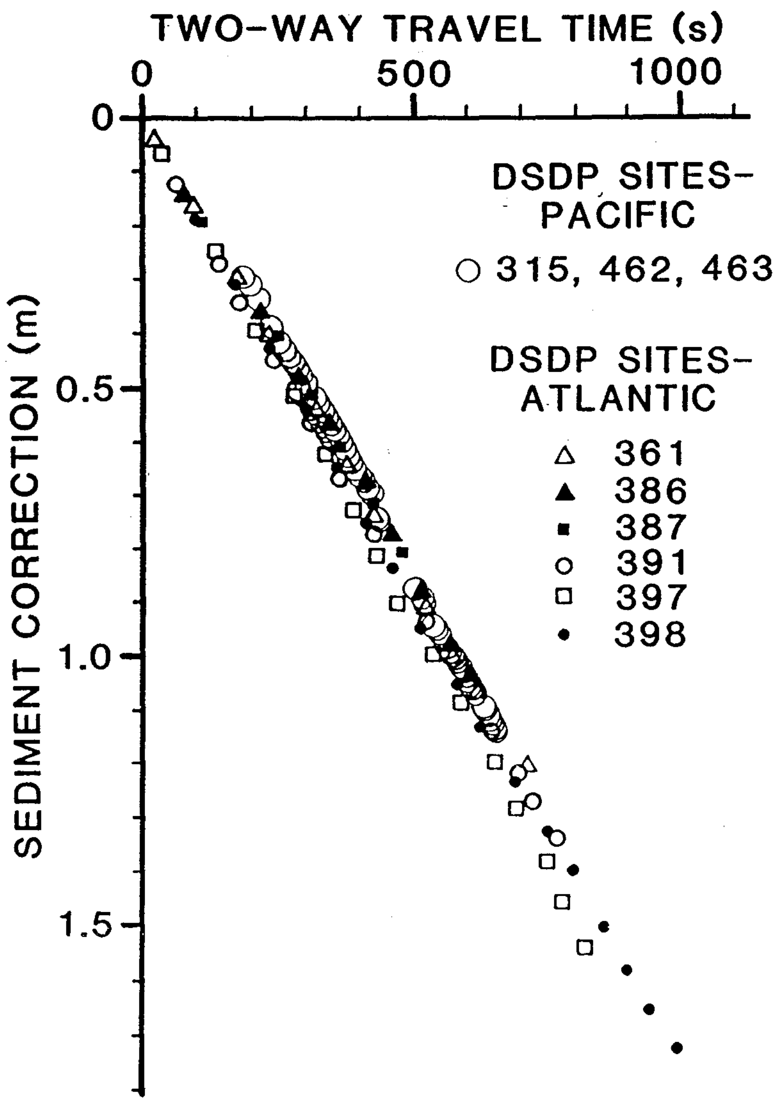

TWO-WAY TRAVEL TIME (s)
0
500
1000
0
0.5
1.0
1.5
SEDIMENT CORRECTION (m)
DSDP SITES-PACIFIC
315, 462, 463
DSDP SITES-ATLANTIC
361
386
387
391
397
398

fig 7

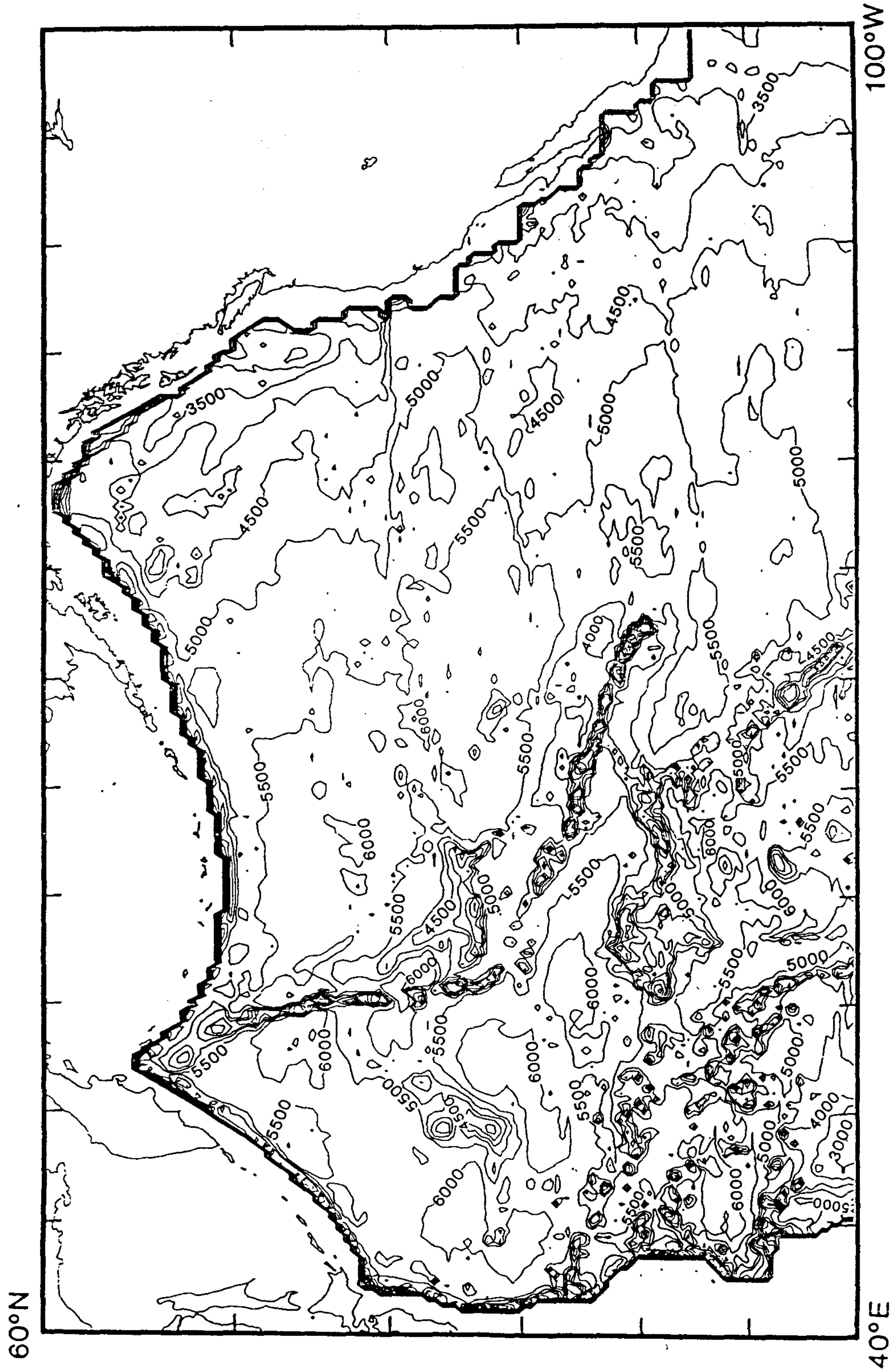

fig 8

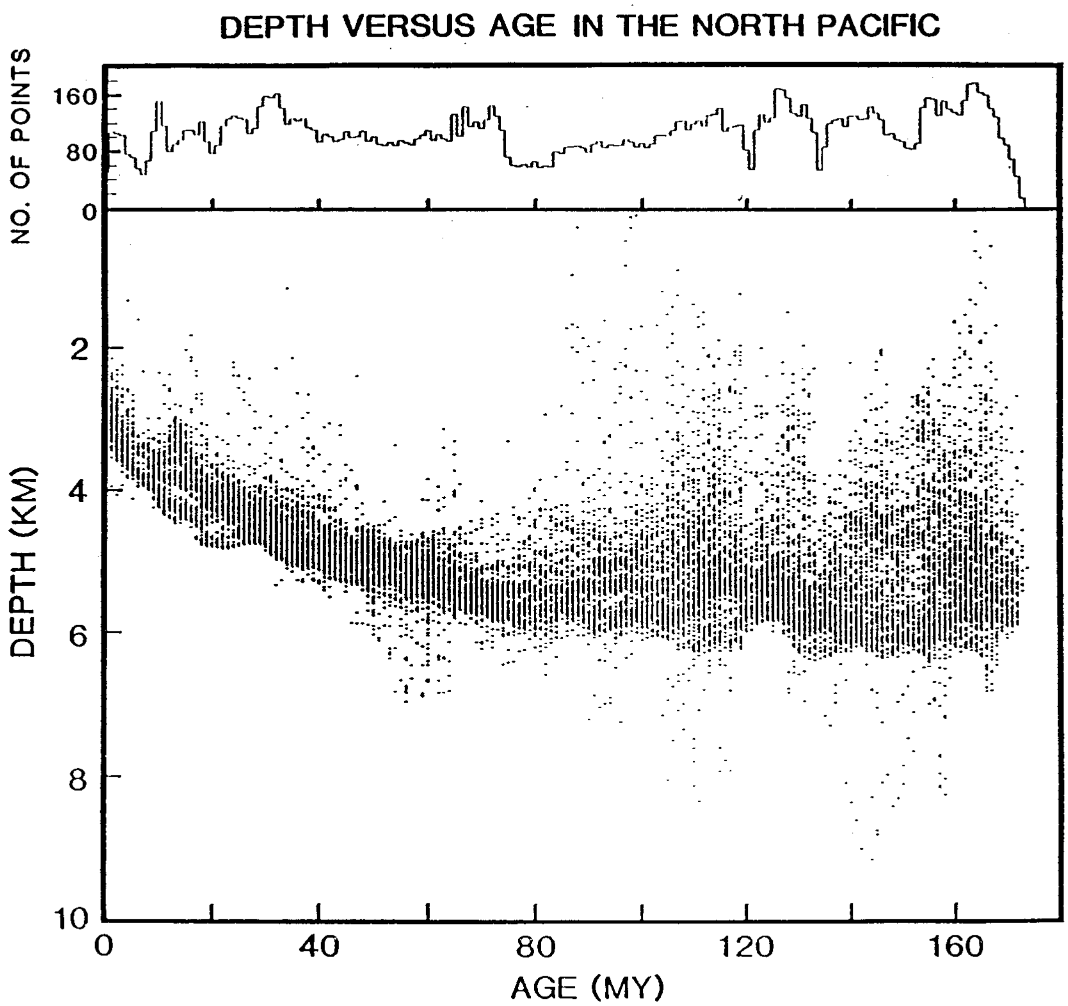
DEPTH VERSUS AGE IN THE NORTH PACIFIC
NO. OF POINTS
160
80
0
DEPTH (KM)
2
4
6
8
10
0
40
80
120
160
AGE (MY)

fig 9

DEPTH VERSUS AGE IN THE NORTH PACIFIC

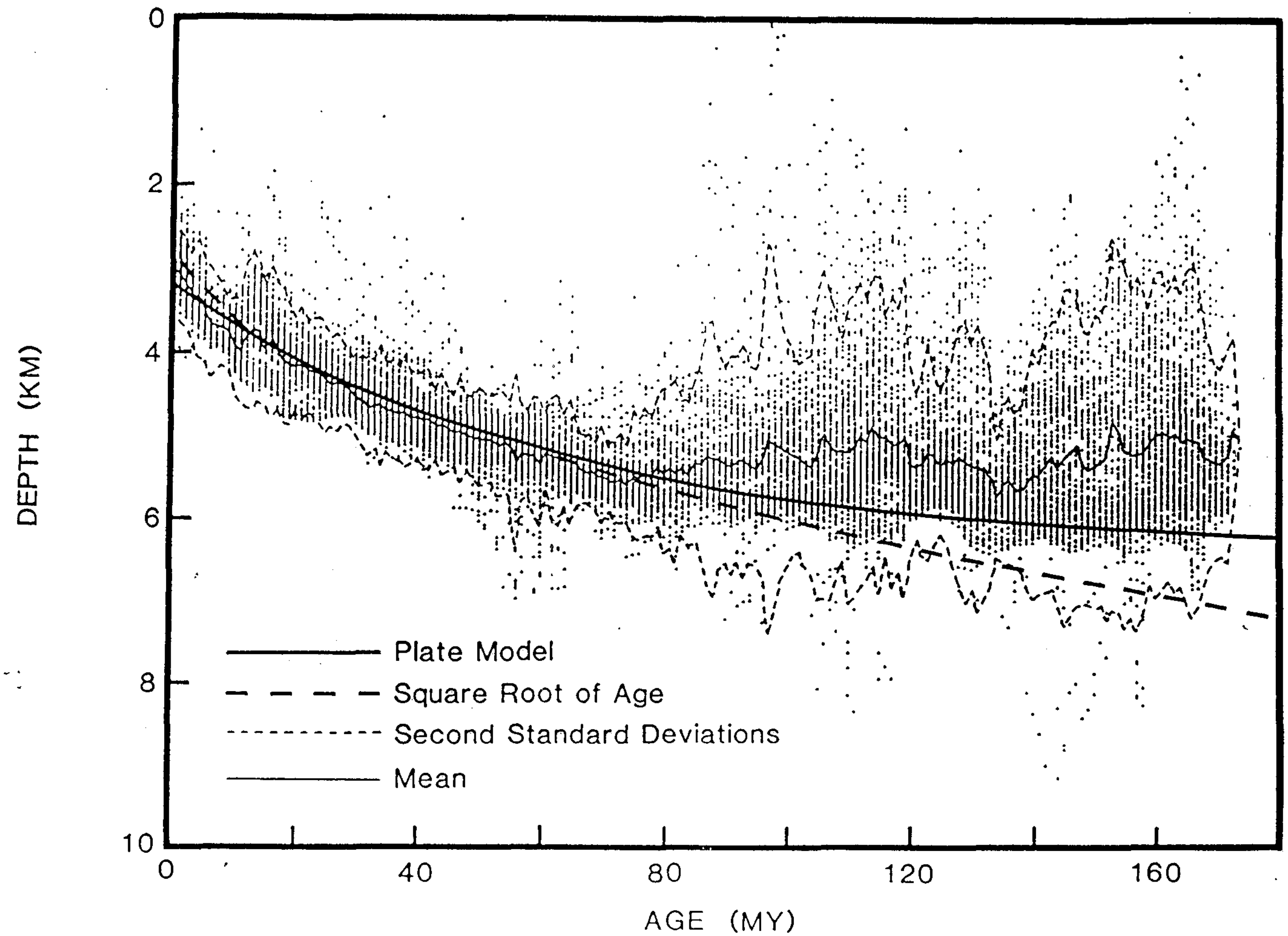

fig 10

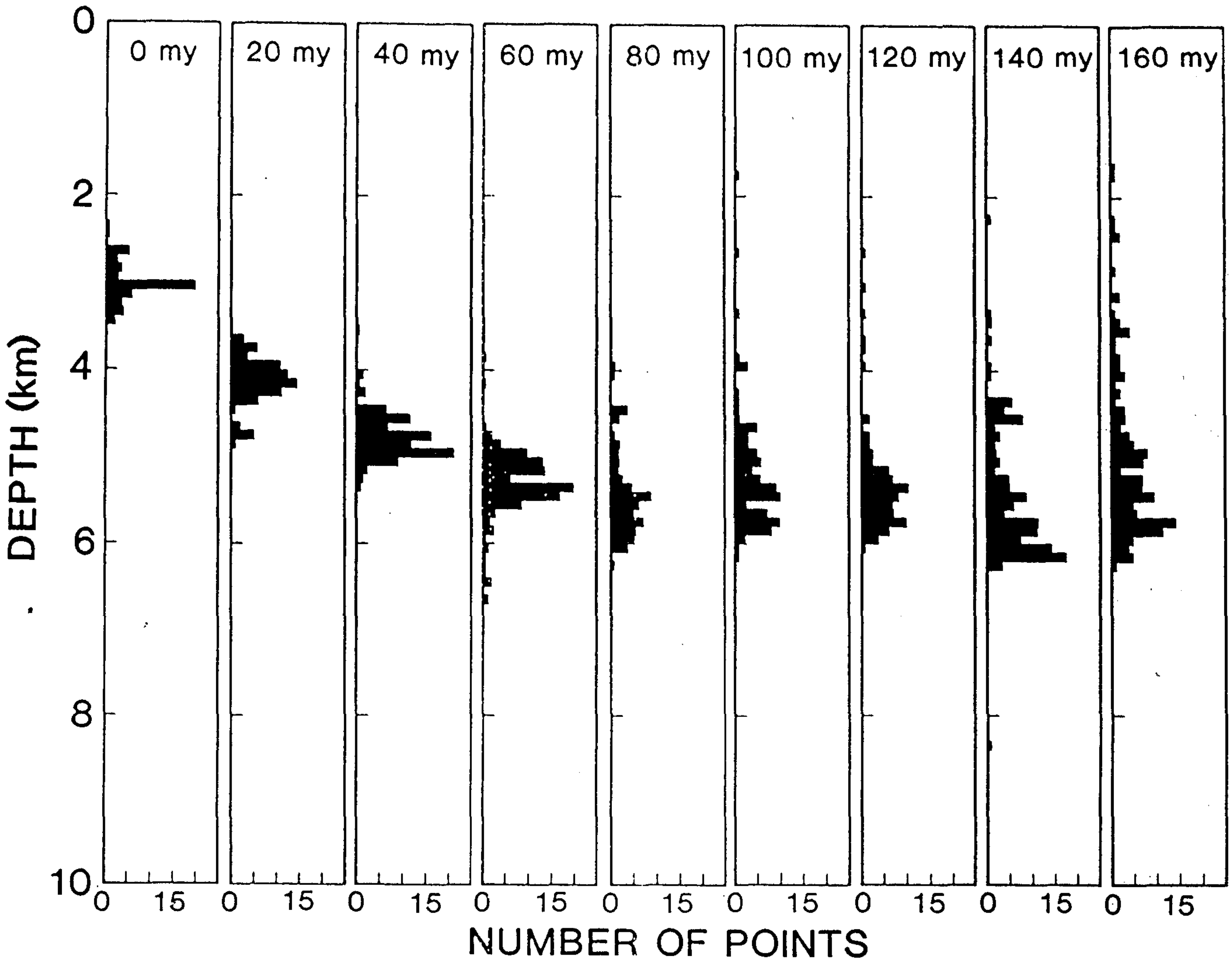
0 my
20 my
40 my
60 my
80 my
100 my
120 my
140 my
160 my
DEPTH (km)
0
2
4
6
8
10
0 15
NUMBER OF POINTS

fig 11

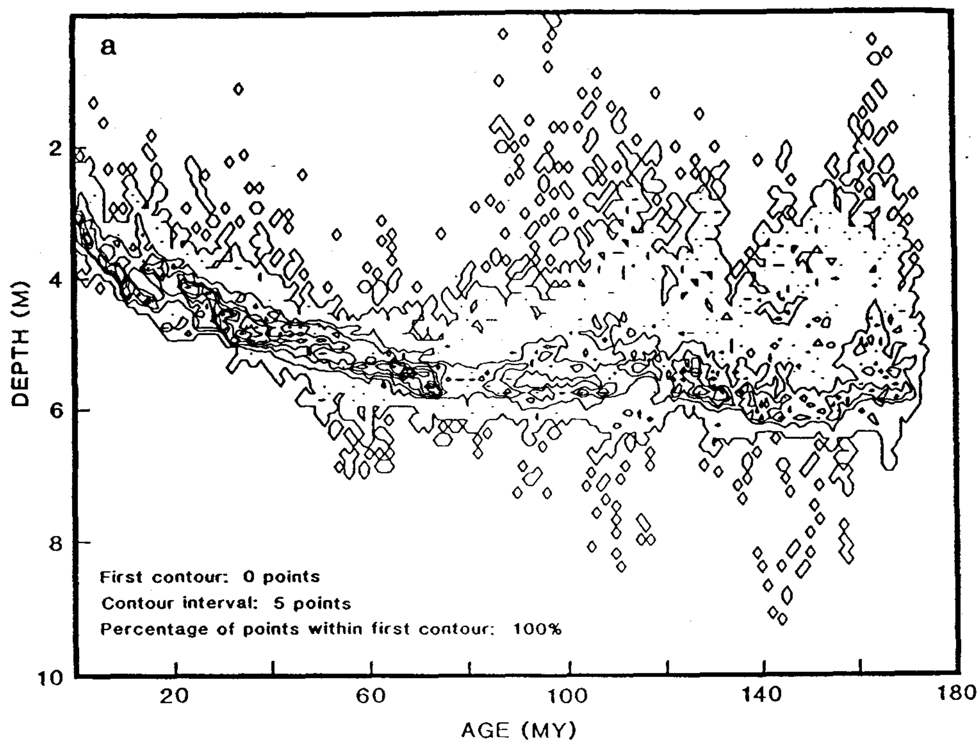
a
DEPTH (M)
2
4
6
8
10
First contour: 0 points
Contour interval: 5 points
Percentage of points within first contour: 100%
20
60
100
140
180
AGE (MY)

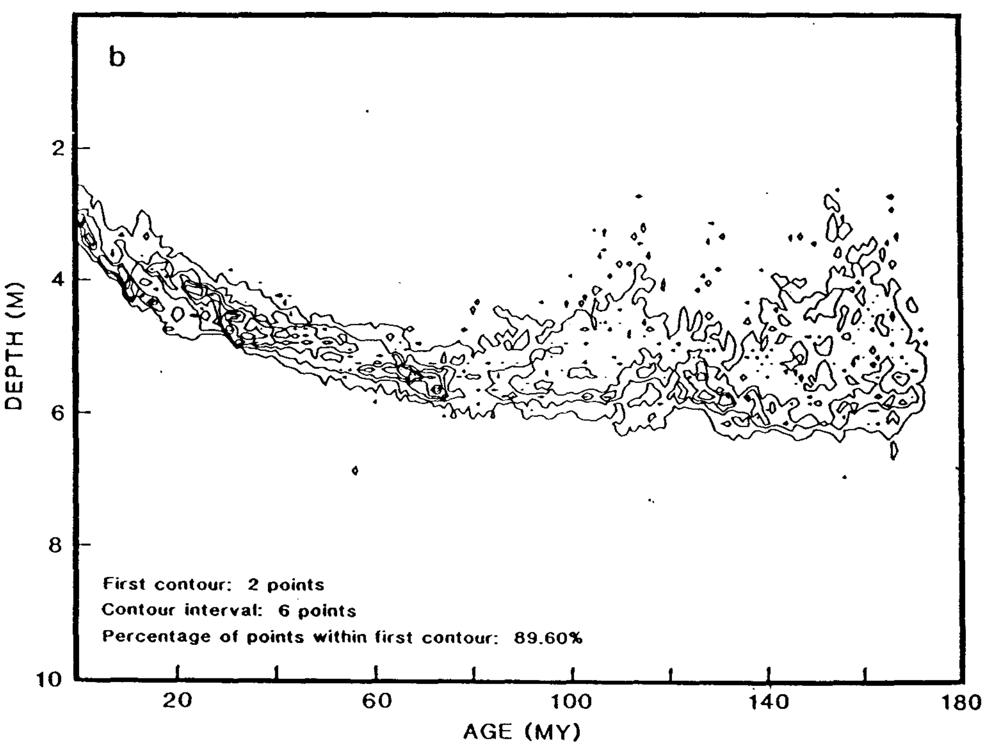
b
DEPTH (M)
2
4
6
8
10
First contour: 2 points
Contour interval: 6 points
Percentage of points within first contour: 89.60%
20
60
100
140
180
AGE (MY)

fig 12

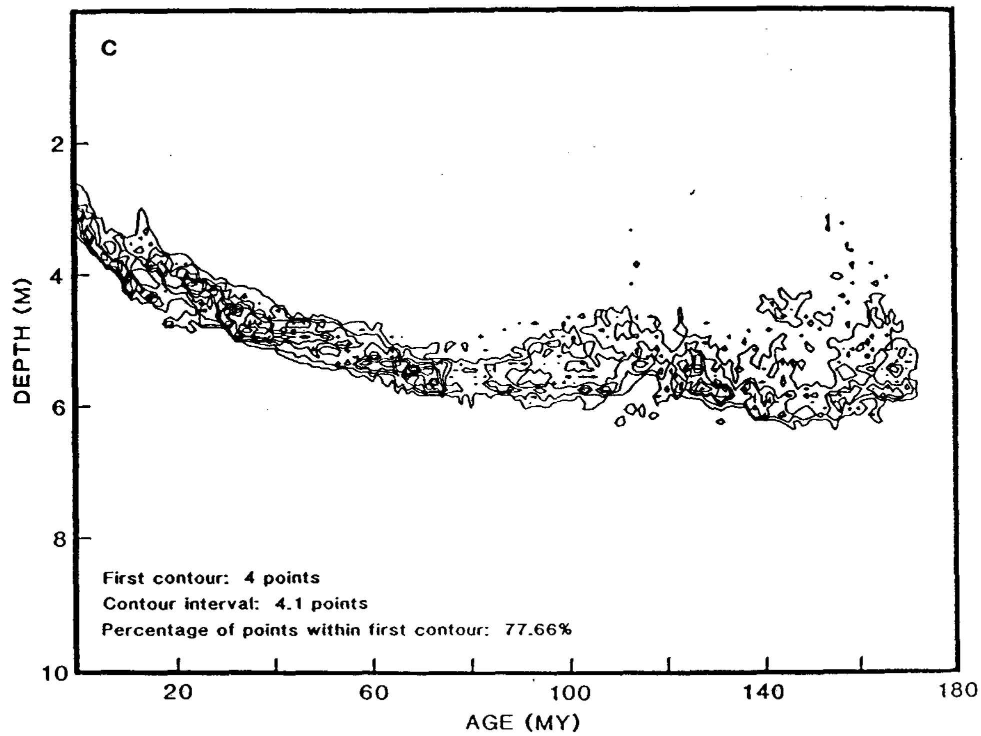
c
DEPTH (M)
2
4
6
8
10
First contour: 4 points
Contour interval: 4.1 points
Percentage of points within first contour: 77.66%
20
60
100
140
180
AGE (MY)

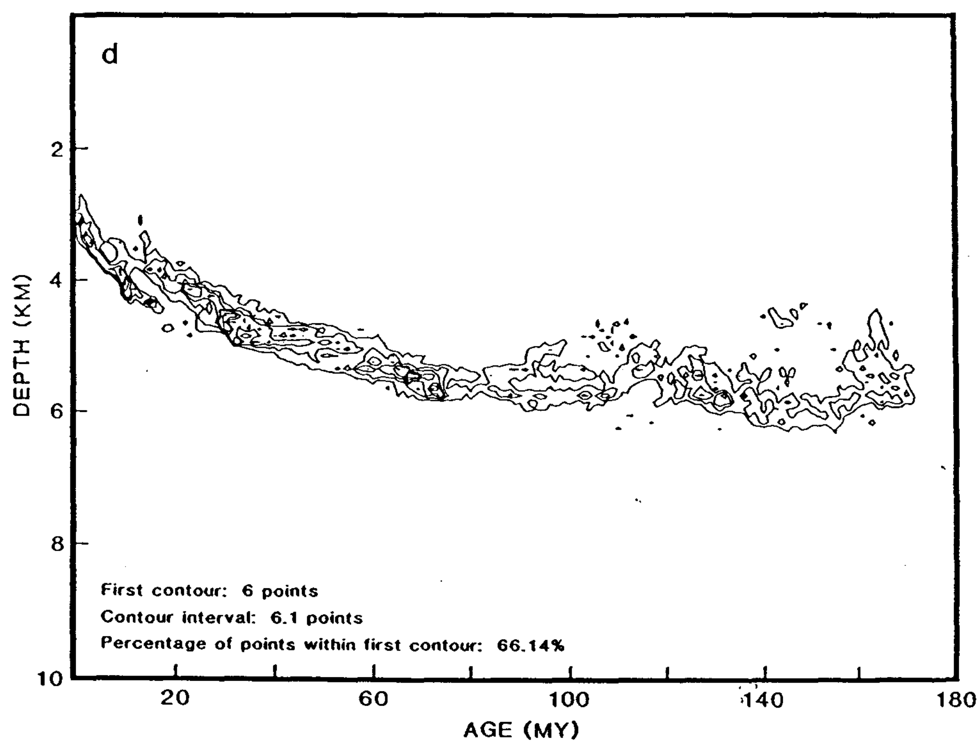
d
DEPTH (KM)
2
4
6
8
10
First contour: 6 points
Contour interval: 6.1 points
Percentage of points within first contour: 66.14%
20
60
100
140
180
AGE (MY)

fig 12 (cont)

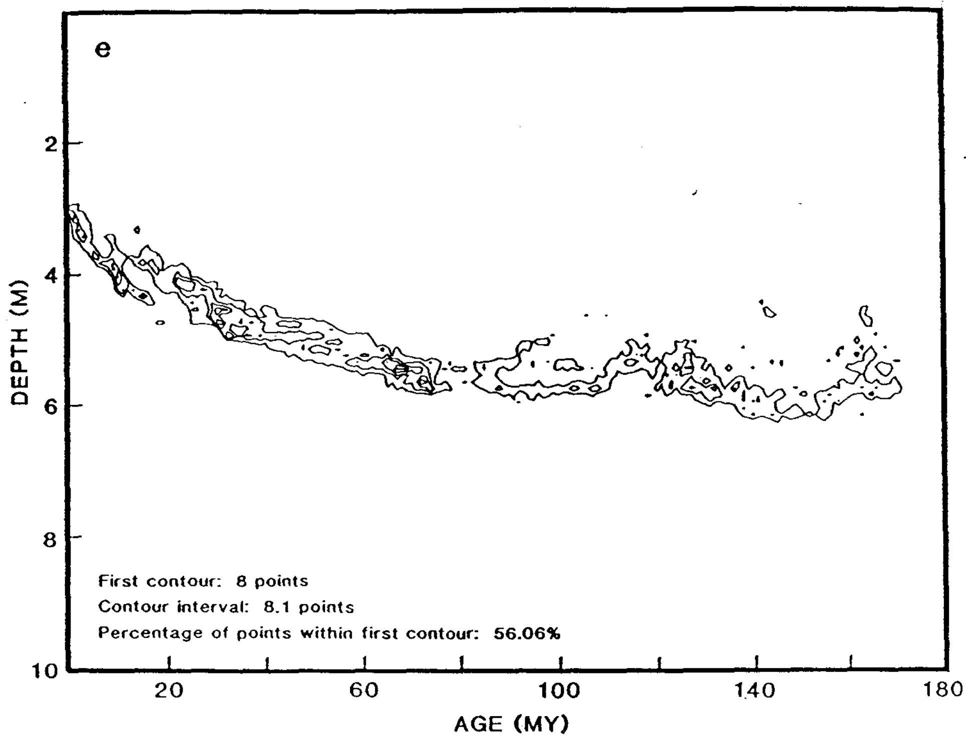

e
DEPTH (M)
2
4
6
8
10
First contour: 8 points
Contour interval: 8.1 points
Percentage of points within first contour: 56.06%
20
60
100
140
180
AGE (MY)

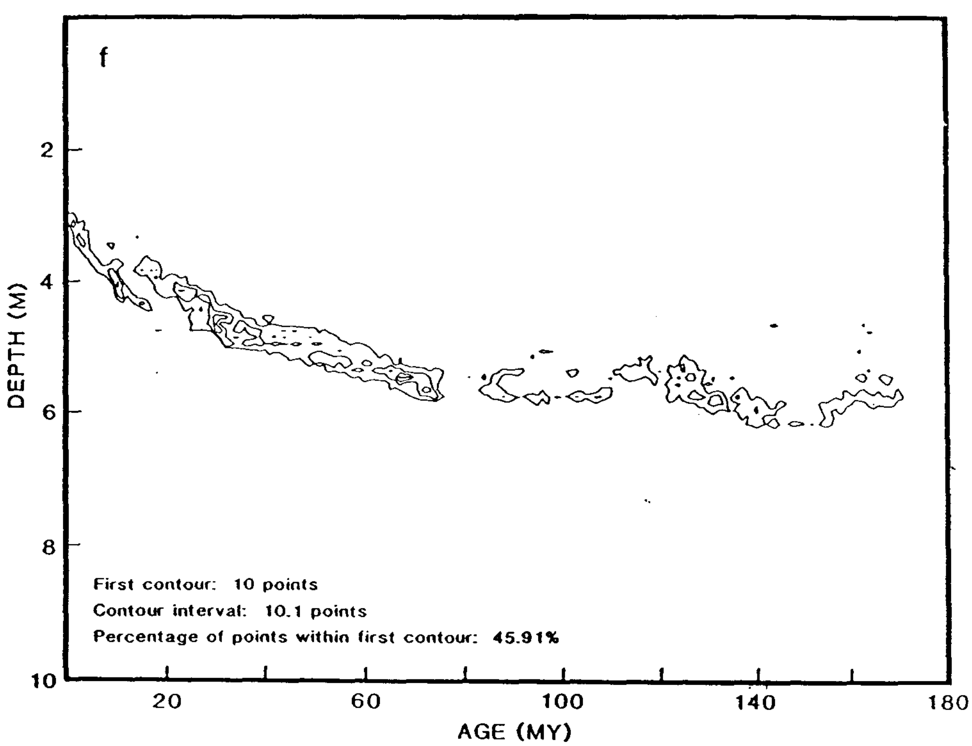

f
DEPTH (M)
2
4
6
8
10
First contour: 10 points
Contour interval: 10.1 points
Percentage of points within first contour: 45.91%
20
60
100
140
180
AGE (MY)

fig 12 (cont 2)

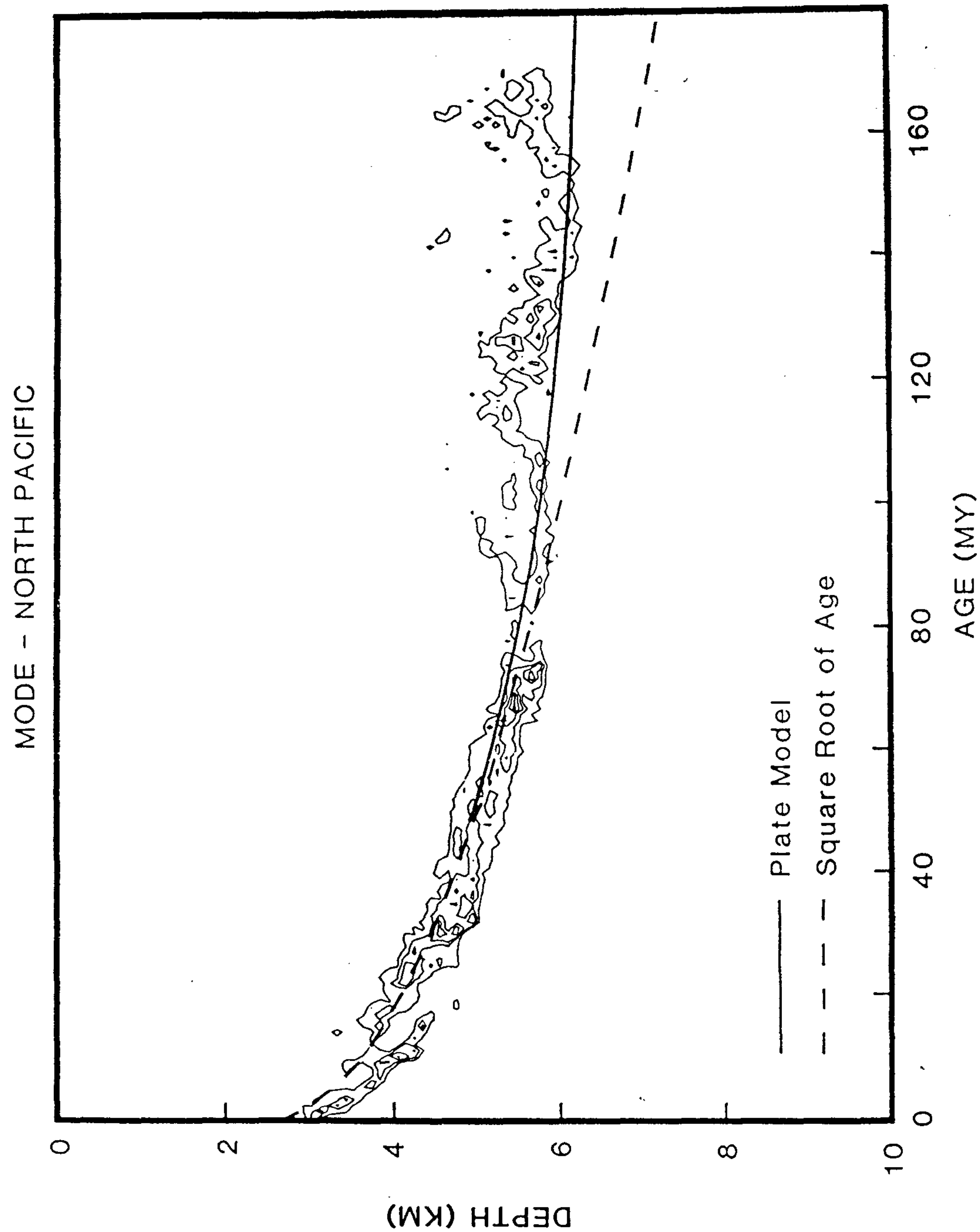
MODE - NORTH PACIFIC
DEPTH (KM)
0
2
4
6
8
10
AGE (MY)
0
40
80
120
160
Plate Model
Square Root of Age

fig 13

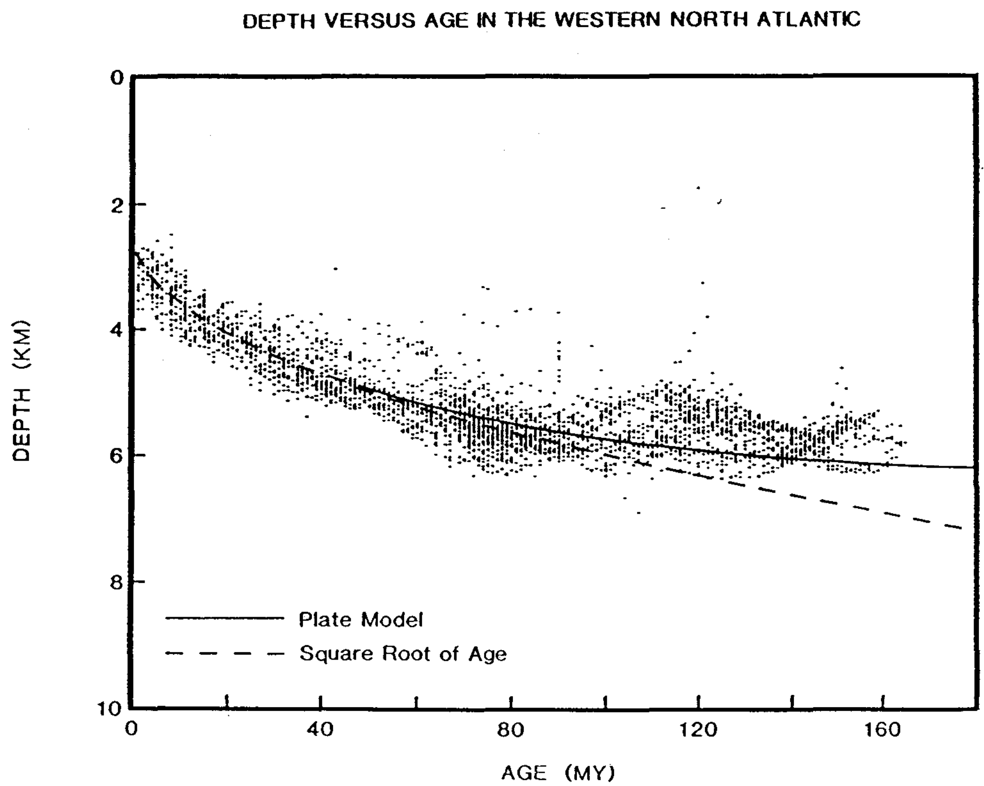
DEPTH VERSUS AGE IN THE WESTERN NORTH ATLANTIC
DEPTH (KM)
0
2
4
6
8
10
0
40
80
120
160
AGE (MY)
Plate Model
Square Root of Age

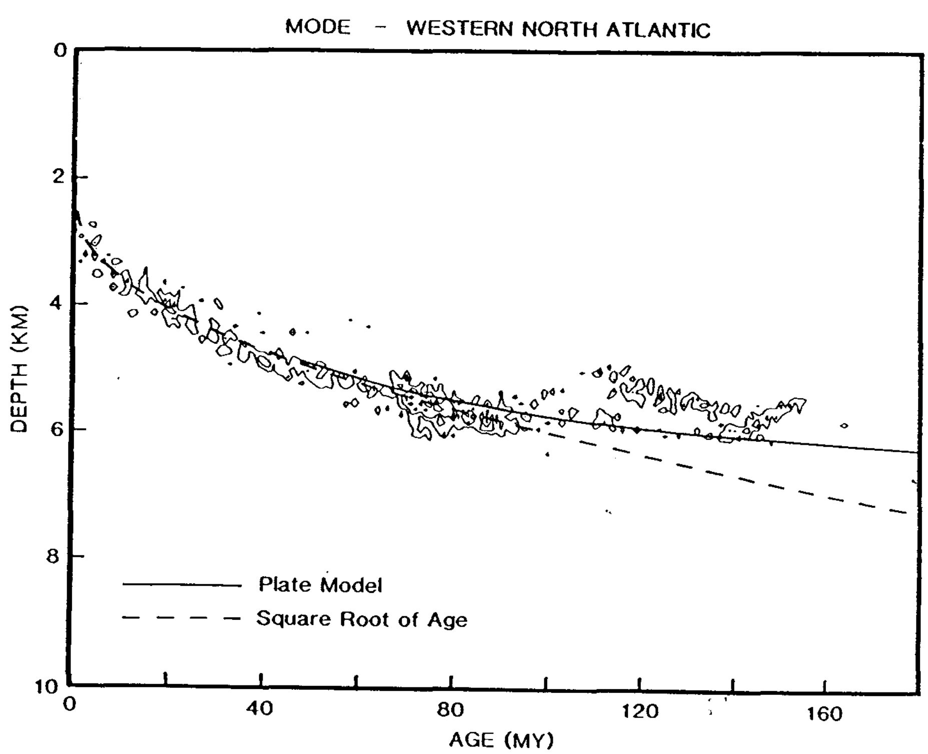
MODE - WESTERN NORTH ATLANTIC
DEPTH (KM)
0
2
4
6
8
10
0
40
80
120
160
AGE (MY)
Plate Model
Square Root of Age

fig 14

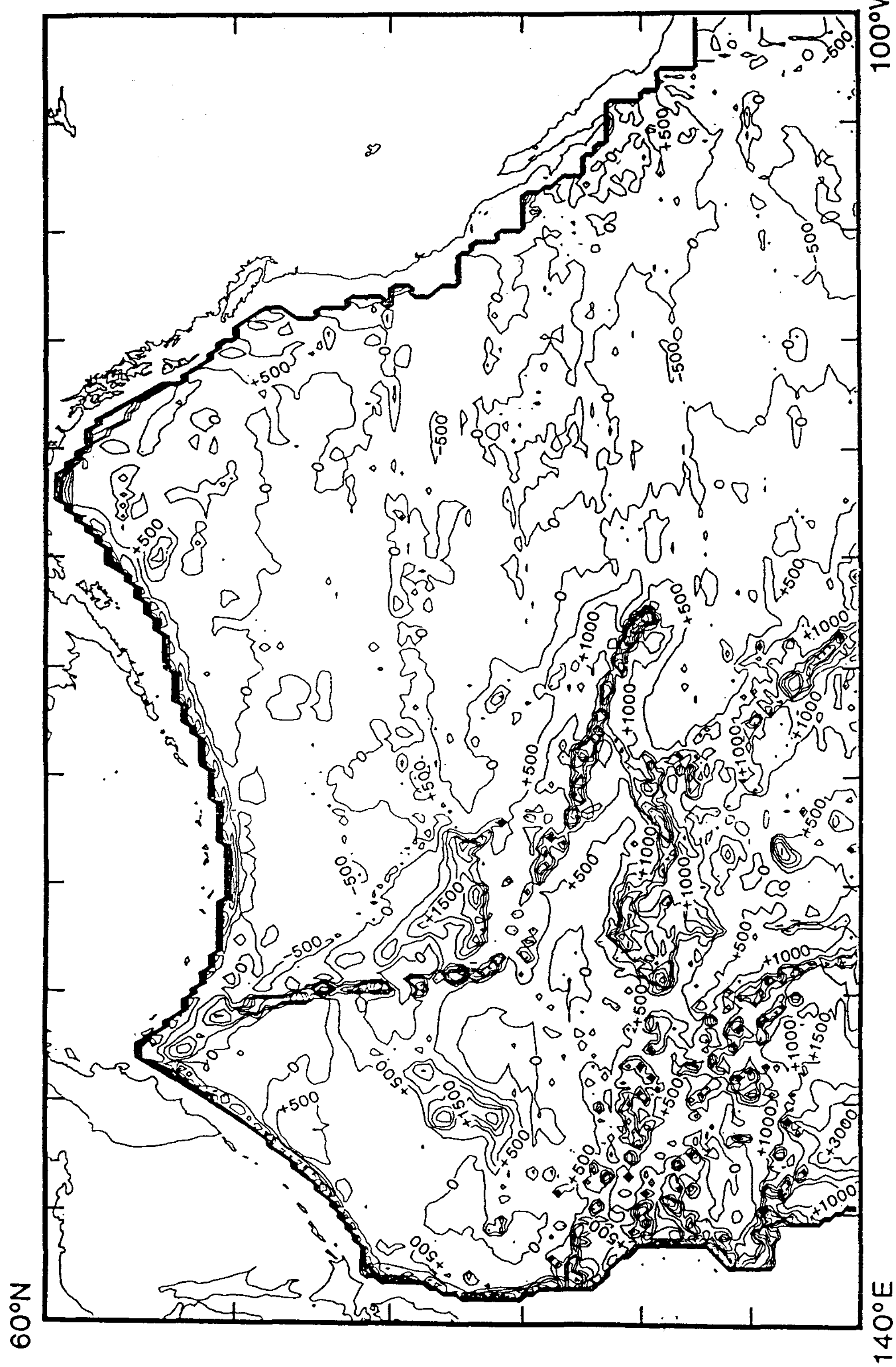

fig 15

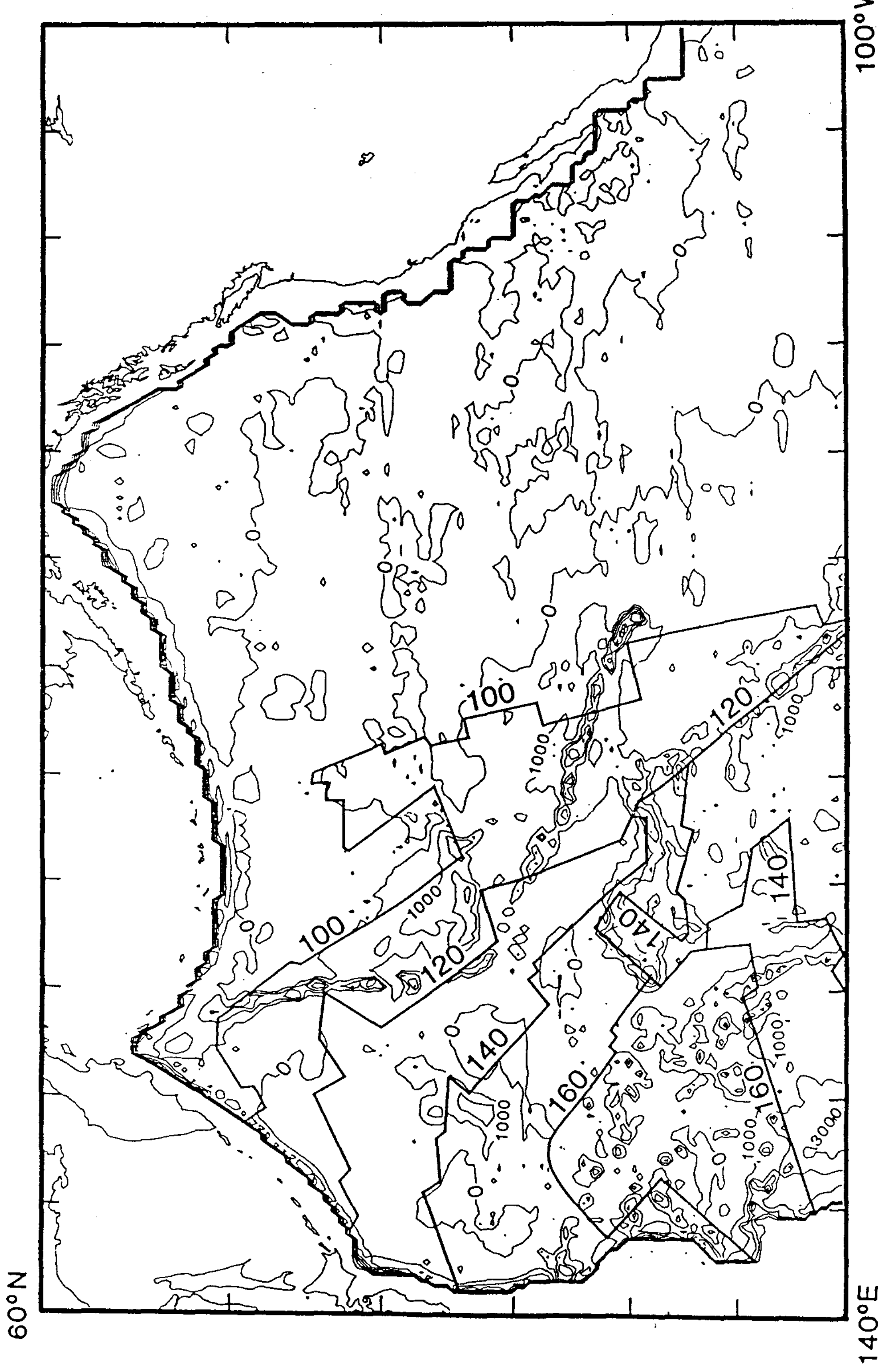

fig 16

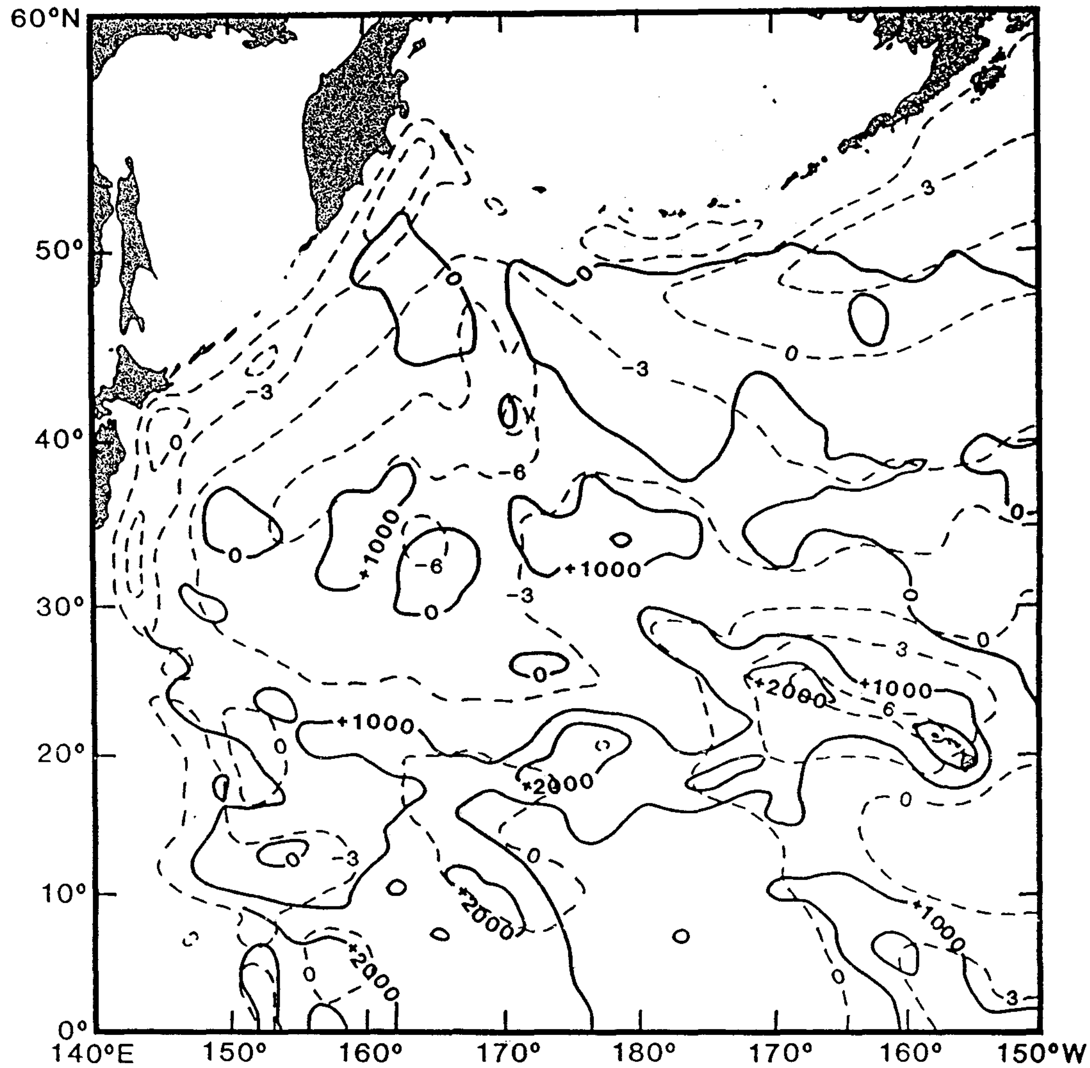

60°N
50°
40°
30°
20°
10°
0°
140°E
150°
160°
170°
180°
170°
160°
150°W
0
-3
-6
3
6
+1000
+2000

fig 17

a

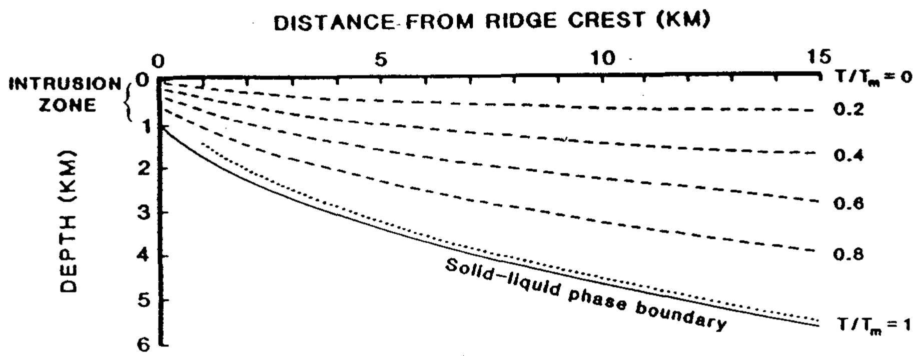
DISTANCE FROM RIDGE CREST (KM)
0
5
10
15
INTRUSION ZONE
DEPTH (KM)
0
1
2
3
4
5
6
T/Tm = 0
0.2
0.4
0.6
0.8
T/Tm = 1
Solid–liquid phase boundary

b

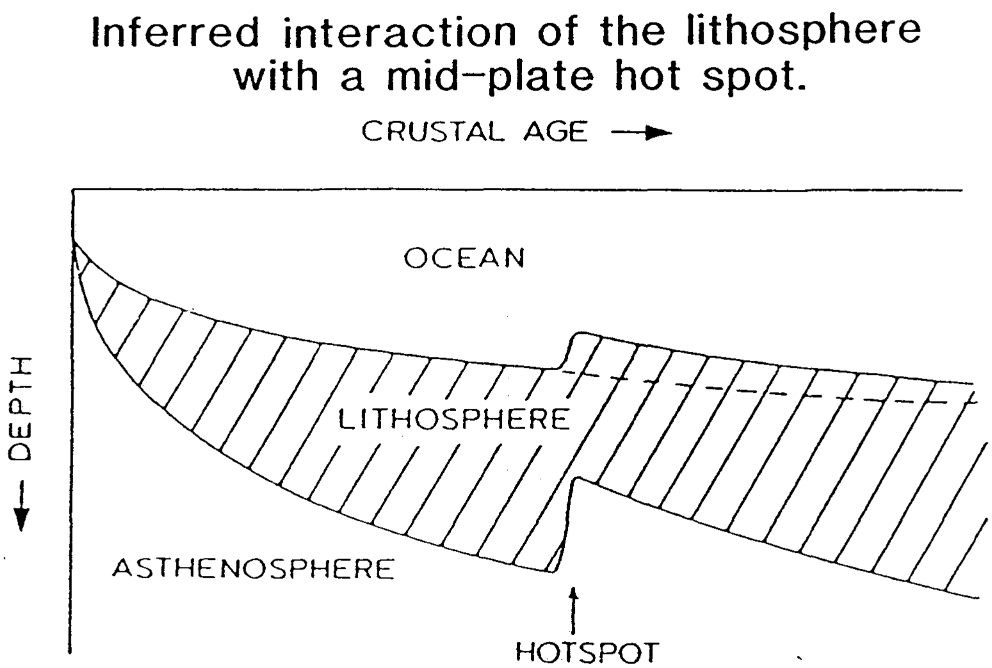
Inferred interaction of the lithosphere with a mid–plate hot spot.
CRUSTAL AGE
OCEAN
DEPTH
LITHOSPHERE
ASTHENOSPHERE
HOTSPOT

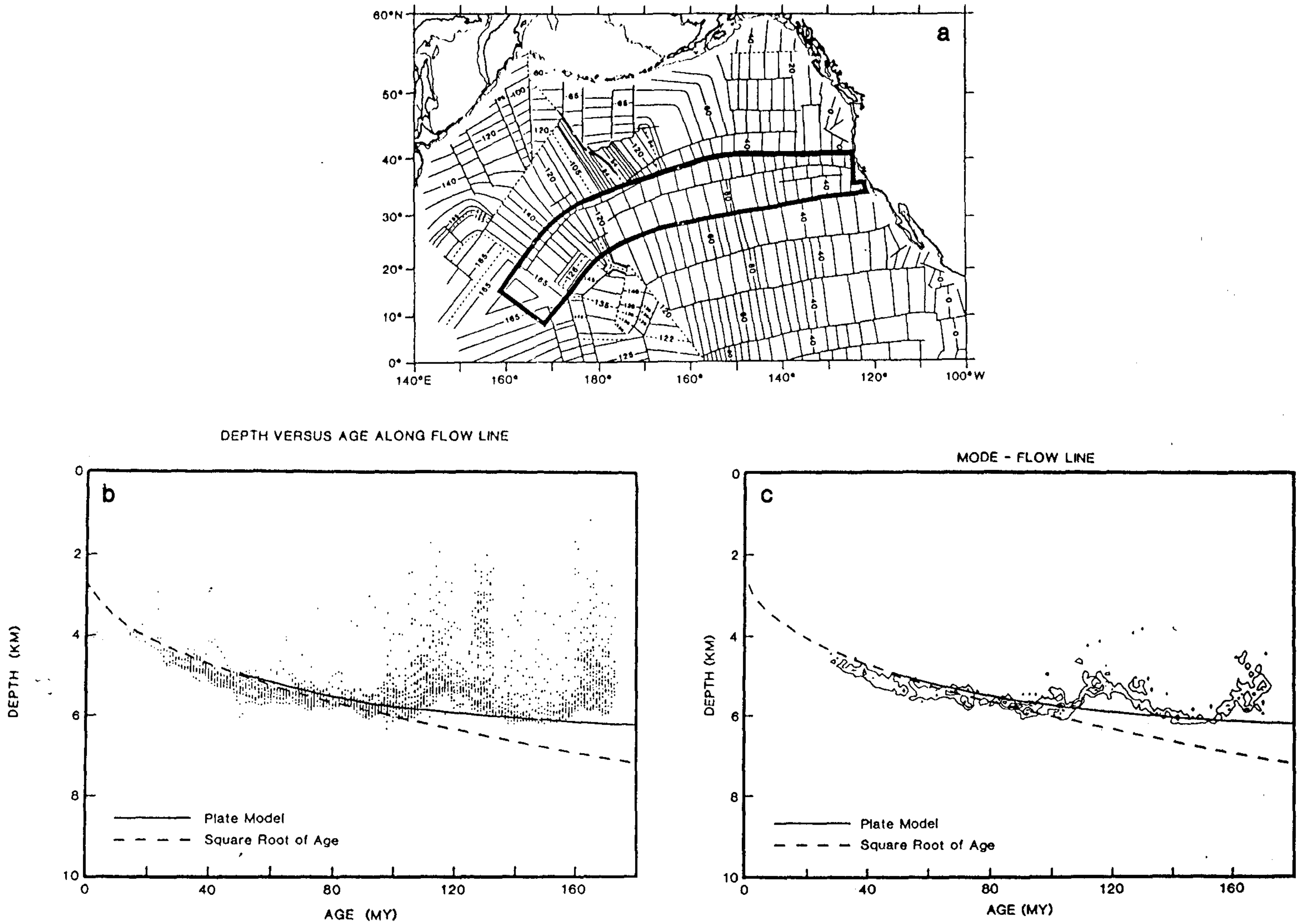
a
60°N
50°
40°
30°
20°
10°
0°
140°E
160°
180°
160°
140°
120°
100°W
DEPTH VERSUS AGE ALONG FLOW LINE
b
DEPTH (KM)
AGE (MY)
Plate Model
Square Root of Age
MODE - FLOW LINE
c
DEPTH (KM)
AGE (MY)
Plate Model
Square Root of Age

fig 19

a

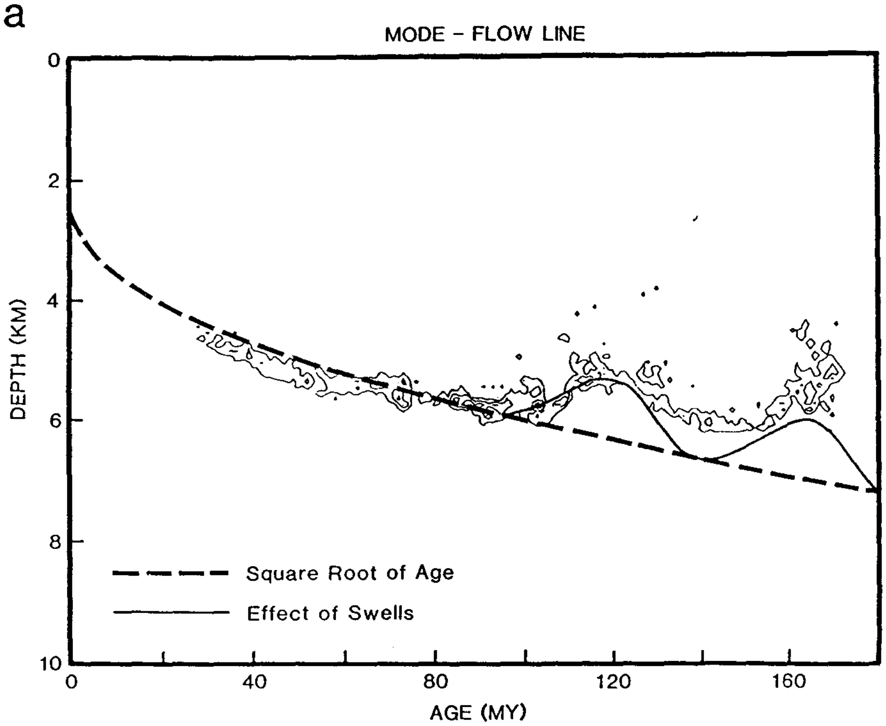
MODE - FLOW LINE
0
2
4
6
8
10
DEPTH (KM)
0
40
80
120
160
AGE (MY)
Square Root of Age
Effect of Swells

b

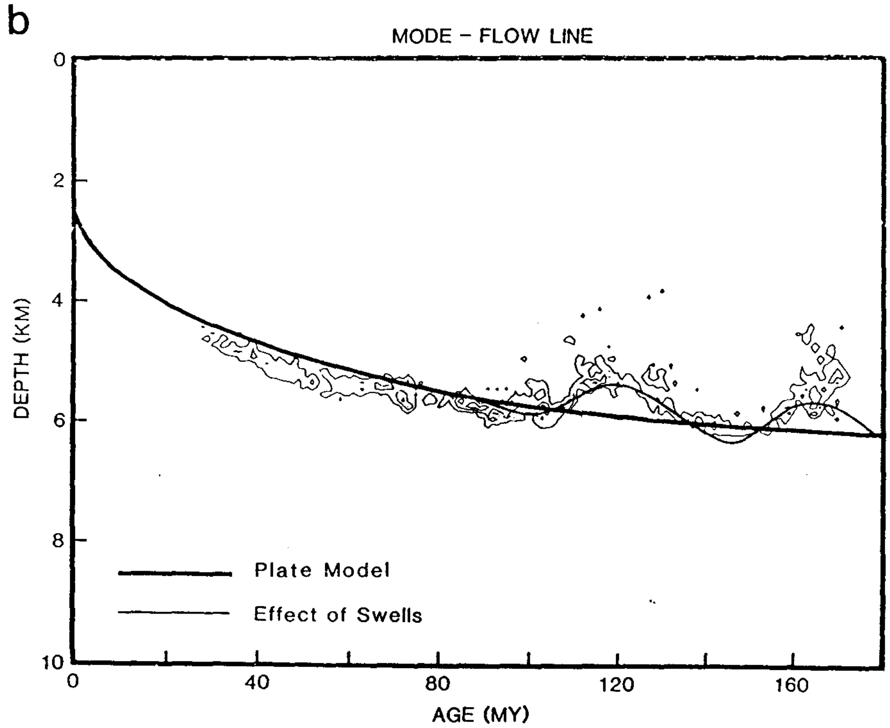
MODE - FLOW LINE
0
2
4
6
8
10
DEPTH (KM)
0
40
80
120
160
AGE (MY)
Plate Model
Effect of Swells

Fig 20

a

IDEALIZED DEVELOPMENT OF AN OCEANIC PLATE

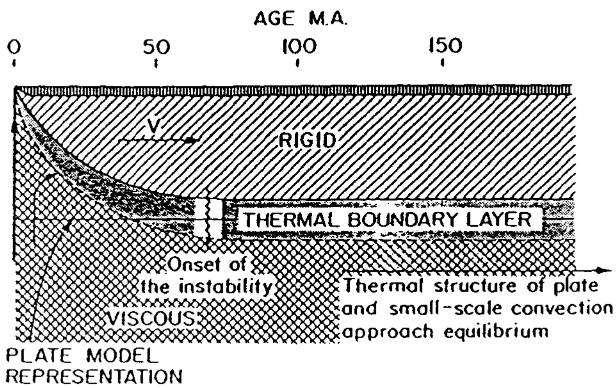

EQUILIBRIUM THERMAL STRUCTURE OF THE PLATE

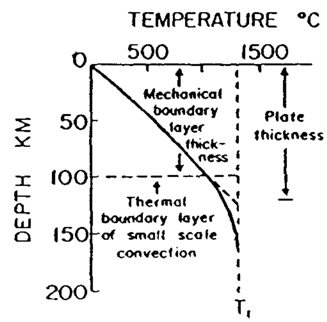

b

Temperature variations within the thermal boundary layer produced by convection beneath the lithosphere.

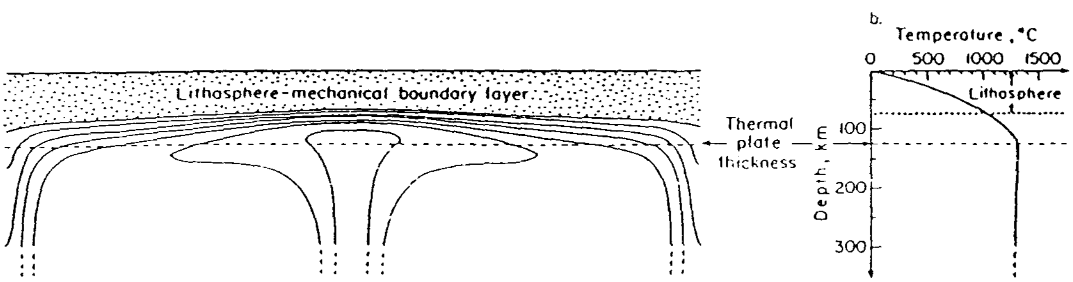

Fig. 21